\

POLITECNICO DI TORINO

Department of Mechanical and Aerospace Engineering
Master's degree in automotive engineering

Master's Degree Thesis

Comfort analysis based on vehicle onboard measurements.

Supervisor

Prof. Alessandro Vigliani

Ing. Carlos Sebastian Nerini

Ing. Antonio Tota

Candidate

Giacomo Vella

Academic Year 2023 - 2024

\

\

Contents

\

\

List of figures

\

\

Abstract

In the last years, the importance of ride comfort is gaining more and more attention in the automotive industry. This heightened awareness has spurred a substantial influx of efforts aimed at enhancing the overall riding experience and a large number of improvements it has been made through qualitative and quantitative test. The purpose of the thesis is to explore the potential of the wheel force transducer and compared the results in time and frequency domain with the more spread accelerometer output.

The aim of this thesis is to provide data by means of experimental analysis and to compare them with different test tracks, in particular, the study includes three test tracks at the Michelin plant in Ladoux, France, where tests are carried out at speeds of 50, 80 and 100 km/h. In addition, evaluations are conducted at the test track in Vairano, Italy, designed for comfort tests. These are tests at speeds between 15 and 55 km/h, with 5 km/h step increments. The tests focused mainly on the longitudinal and vertical dynamics of a fully instrumented Alfa Romeo Stelvio, it should be noted that the instrumentation used was to investigate the handling of the car. moreover, the analysis has been done when all the data were already collected, without the possibility to do more tests. The outputs were also computed followed by signal processing using MATLAB software.

Results suggest that the Wheel Force Transducer have significant potential and can provide a type of data with a different information content than the current state of the art that could be led to further enhancements on the ride comfort analysis. A possible weak point could arise from possible measurement errors due to careless mounting for this type of application, as this type of sensor is not specifically designed for this type of test. For this reason, future studies could be carried out by increasing the speed range at which the test tracks are travelled, in order to verify the behaviour obtained in this thesis and, by means of suitable planning, more studies in the frequency domain could be explored.

\

\

Chapter 1

Introduction

1.1 Comfort description

Over the years, achieving ride comfort has posed a considerable challenge in the automotive industry. Despite the highly competitive nature of the market and the impact of numerous environmental and safety regulations, comfort remains one of the most significant elements in attaining customer satisfaction. One of the main reasons for this shift in perspective lies in the growing awareness of the importance of comfort for the health and well-being of both drivers and passengers. The increase in time spent on the road due to traffic congestion and hectic lifestyles has led to a greater focus on the need to create environments within vehicles that reduce stress and improve the quality of time spent in the car. Moreover, battery electric vehicles are becoming more spread and, since the powertrain is much less noisy compared with the ICE vehicles, it is now crucial to reduce as much as possible the noise due to vibration at critical frequencies. Because of that, the importance of understanding and analysing deeply the vibrations mechanisms both in time and frequency domain is increasing attention in the automotive field.

Recent developments in automotive comfort include the integration of advanced suspension systems that reduce vibrations and improve vehicle stability, ergonomic seats designed to reduce fatigue during long journeys, and climate control technologies that maintain optimal internal temperatures. Additionally, connectivity and infotainment within vehicles are becoming more sophisticated, offering occupants a wide range of entertainment options and personalized control.

\

In conclusion, the study of comfort for passenger vehicles is no longer a luxury but a necessity that is driving the evolution of the automotive industry. The challenge for manufacturers is now to balance the demands for performance, safety, and efficiency with consumers' desire for a more comfortable and enjoyable driving experience. This evolution in the automotive landscape underscores the increasing importance that comfort has taken in shaping the future of cars. Because of that growing of comfort research, also the sensors used to investigate the dynamics are becoming more complex and are trying to reach the highest performance. In this work thesis the performance of the Wheel Force Transducer is analysed on different track and at different velocities, the post-processing has been done both in time domain and in frequency domain.

1.2 State of the art

In the realm of automotive design, the pursuit of occupant comfort has become a paramount concern, reflecting a growing acknowledgment of the profound impact comfort exerts on driver and passenger experiences. As vehicular technology evolves, the understanding of comfort extends beyond traditional ergonomics, encapsulating a holistic integration of sensory, psychological, and physiological factors. This literature review aims to navigate the landscape of comfort research within the automotive industry, exploring key dimensions, recent advancements, and challenges that define the current state of knowledge, focusing on the testing features, with the description of the different approaches and evaluating the adopted sensor in order to acquire state-of-the-art methodologies. Thus, İ. Karen et al. [1] implemented on four different vehicles several accelerometers to collect the necessary data to parametrize the most important system that has to comply with comfort, the suspensions. The cited paper encompasses two distinct physical tests to facilitate a comprehensive analysis of ride comfort. The initial test is designed to procure essential data for calculating the ride index, while the

\

second test focuses on gathering fundamental parameter values crucial for the subsequent modelling phase of the full-car simulation.

To conduct these tests, four vehicles were deliberately selected, comprising two medium sedan passenger cars and two light commercial vehicles. This deliberate selection allows for a comparative assessment of ride index variations between different vehicle types and an exploration of the relationships within the same vehicle types. Concurrently, the choice of six diverse roads, each with distinct properties such as asymmetric traverse, dirt road, paved surface, highway, test track, and patched road, is made to serve the same dual purpose of vehicle selection.

The highway road test introduces velocity as a variable, examining the impact on ride comfort at two different speeds (100 and 140 km/h). In this context, 19 accelerometers are strategically positioned on each vehicle, capturing acceleration values through two signal collectors, resulting in a total of 41 channels. Fig. [1] illustrates the planned accelerometer locations, excluding the engine region.
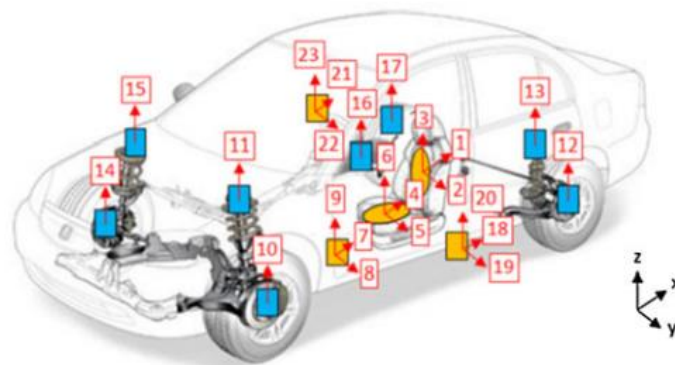
Figure 1, Accelerometers placement.

Within the suspension system, eight accelerometers, each with a single channel along the z-axis, are placed. The engine, a focal point of investigation for its effects on ride comfort, features six accelerometers three on each mount with a total of 18 channels covering x-, y-, and z-axes. Moreover, to measure vibrations on the seat surface conveniently, a seat-pad equipped with an accelerometer is utilized, providing data

\

through three channels. This meticulous instrumentation and testing methodology contribute to the comprehensive exploration of ride comfort and the intricate dynamics between vehicle components, thereby enhancing the overall depth of this study. Furthermore, Thom B. et al [2] aim to give their contribution to the overall analysis for ride comfort evaluations through the Source Path Contribution (SPC), very helpful technique Deployed for comprehending the distinctive attributes of individual sources and the pathways that amalgamate towards a receiver location, this analysis entails a thorough characterization of each source. This characterization process involves leveraging operational measurements, local transfer functions, and global transfer functions, all integrated to arrive at receiver locations. The integration of these terms facilitates a holistic understanding of the cumulative impact of each partial contribution emanating from instrumented locations on the receiver locations [3]. In order to carry out the described research, the vehicle was again instrumented with accelerometers, but they were not the only sensor, in fact in this case it has been used several strain gauges to measure forces at specific locations. In the assessment of the system, a single passenger vehicle underwent instrumentation with transducers strategically placed at points where input forces were applied to the body. The sources considered in this study encompassed suspension points at all four corners of the vehicle and every powertrain mount. Suspension sources involved control arms, dampers/springs, and stabilizer bars. Each of the source locations (amounting to 26 in total) was locally instrumented with three linear strain gauges and two triaxial accelerometers. This latest academic paper once again refers to the state of the art, highlighting the widespread use of accelerometers to conduct research in the field of automotive comfort, confirming almost entirely the non-use of the WFT on this topic. The explanation for such sparse use of wheel force transducers is surely due to practical cost factors, in fact they are extremely expensive sensors compared to the prices of common accelerometers. In addition, the implementation on the vehicle to be tested involves more mechanical steps to replace the wheel. This process is particularly critical, as the assembly must be carried out with great care, in order to avoid possible errors in the measurements.

\

Lastly, as highlighted by Burkard H. et al [4] the WFT has the undesired effect of changing the unsprang mass of the suspension system, leading to possible changes of the overall dynamic behaviour of the suspension system, "breaking" the known rule that suggest leaving the characteristics of the vehicle as unchanged as possible. As described in their work, every existing WFT system alters the unsprang mass, inertia, and stiffness in comparison to the standard wheel. It is imperative to quantify and assess these influences to determine their significance within the specific field of application under consideration. In addition, the tire characteristic, kinematic and geometric effects due to suspension design, and changing the sprung mass could change also the behaviour of the tire under specific circumstances. Towards the improvement of the evaluation and the application of dynamic load measurements on real road surfaces it is desirable to have as much quantitative information on the effects of these parameters as possible. It must be highlighted that the tested vehicle travelled on public roads. The reaction forces are contingent upon the masses, stiffnesses, and inertia moments of all involved components. Consequently, the forces exerted by a particular section of the road surface are reliant on vehicle-specific parameters. Additionally, the speed of the vehicle evidently contributes to the modulation of these forces. In the end, the conclusions highlight that the influence of the WFT plays an important role on the acquired data and the authors suggest that it could be beneficial for WFT vendors and implementers to collaborate on a collective program aimed at gaining a deeper understanding of how various parameters impact the precision of dynamic wheel load measurements. Further investigation on changing the sprang mass is reported by Shawn S. You [5], that focuses his work on studying and especially comparing the data collected from three different cars, 2 medium class sedan and a SUV, with and without the WFT. He highlighted once more that, since the vehicle is a spring mass damper system, a change in the stiffness, mass, and/or rotary inertia may change vehicle dynamic response, therefore affecting measurements. Particular interest was placed on the frequency analysis carried out by the author. As it can be seen from Fig. [2] there

\

are few differences between the system with and without the WFT, especially on the amplitude changes at around 25 Hz. The alterations resulting from the additional
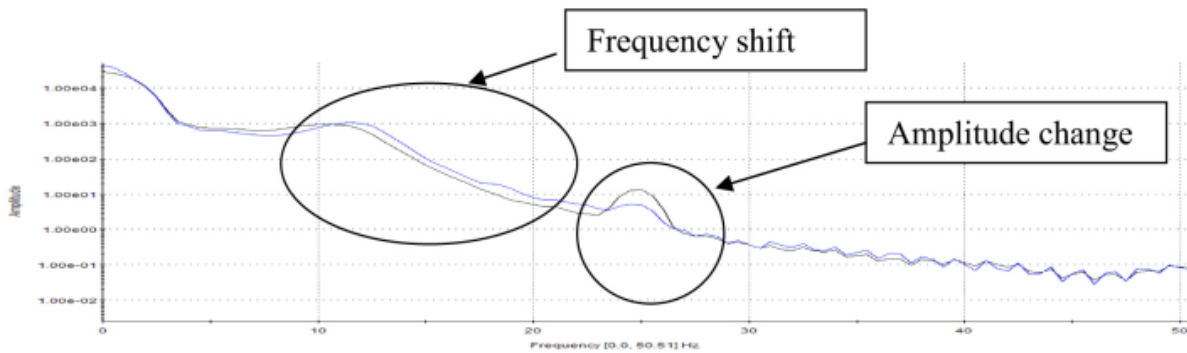
Figure 2, Car 1, sedan. Black with WFT and blu Without.

mass led to shifts in resonance frequency and amplitude. This observation indicated that the vehicle's modal response was influenced by the introduction of added mass. In the case of both passenger cars, the added mass tended to have a more detrimental effect, while for the SUV, the impact of the added mass was comparatively less damaging. Analysis of pseudo damage distribution revealed that, in the presence of added mass, damage levels for acceleration signals were generally lower compared to situations without added mass. Conversely, the percentage of damage for strain exhibited an opposite trend. In the end, the effect of added mass of WFT was very vehicle dependent and location dependent.

Therefore, the application of WFTs is particularly scarce and there are only a few academic articles dealing with the subject. this thesis project therefore aims to explore the performance of this sensor, taking into account the limitations present, such as, for instance, the impossibility of conducting further tests and being able to plan them accurately, and aiming to demonstrate specific aspects.

\

1.3 Work Frame

Firstly, it should be highlighted that all the data used in this project come from the tests done by the "Vehicle Interaction Measurement Research Project" at the test tracks of Ladoux (FR) and of Vairano (IT). The car used in both cases was an Alfa Romeo Stelvio, instrumented with several sensors capable to capture all data required.
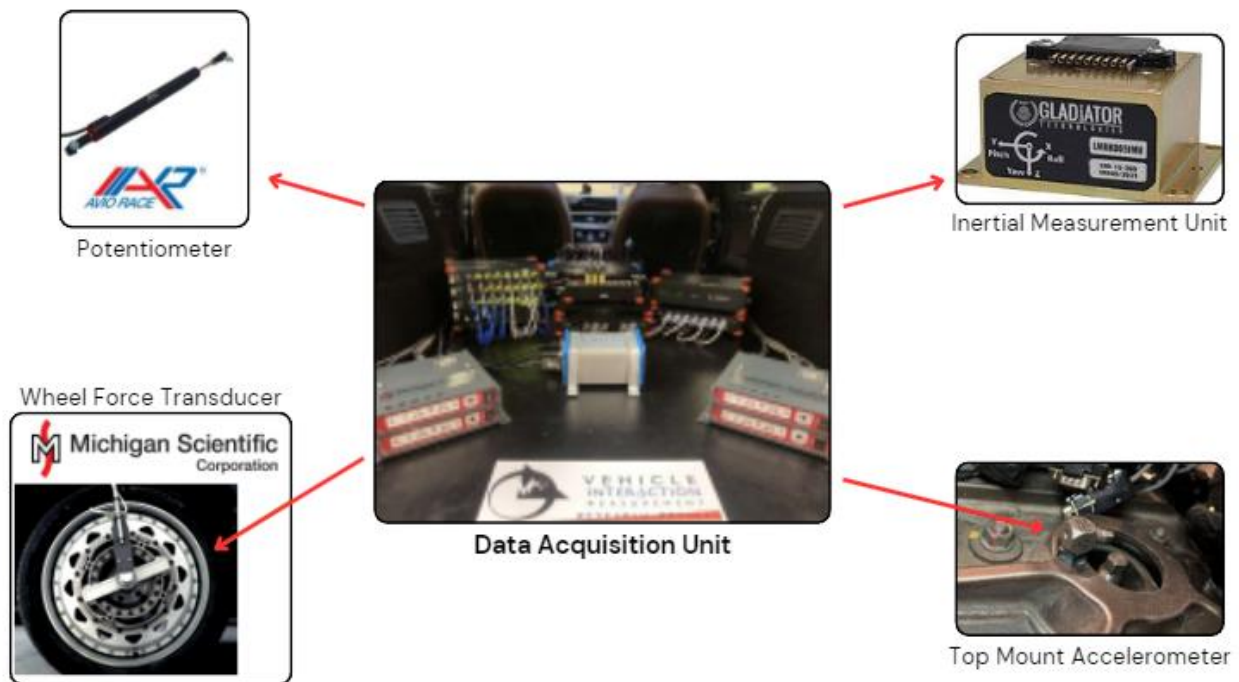
Figure 3, Vehicle instrumentation.

In this research, the performance of the Wheel Force Transducer produced by "Michigan Scientific Corporation" has been analysed and compared with the performance of the accelerometers provided by "Kistler". The accelerometer measurements were available only in Ladoux test track. The accelerometers were mounted in different location of the vehicle:

- Wheel Hub (all wheel)
- Top Mount (all wheel)
- Seat base

\

and, thanks to that it was possible to better analyse the behaviour of the vehicle from the wheel to the seat base, following the transmission path of the main vibrations that typically arrives to the passengers.
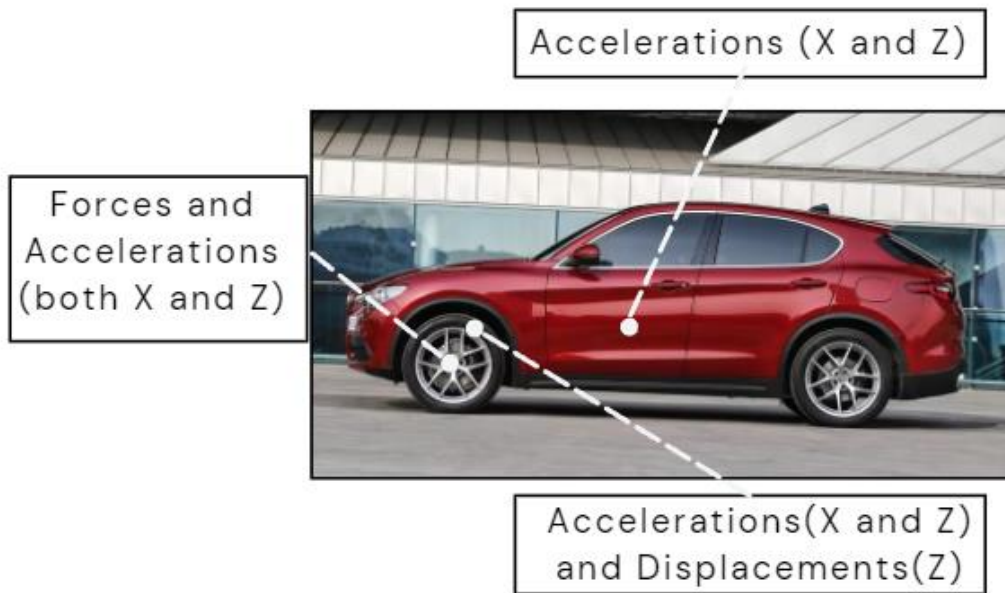
Figure 4, Case study, sensor placement.

The Ladoux (FR) and Vairano (IT) tracks were selected to evaluate vehicle longitudinal dynamics performance because they both have dedicated "Lines" for comfort studies. The French track offered three different lines, with various distributions and types of obstacles, travelled at three different velocities: 50, 80 and 100 kph. While, Despite the presence of only one comfort line on the Vairano route, this was chosen for its suitability for the project. The line was driven at different speeds, varying from 15 kph to 55 kph in increments of 5 kph. This step-by-step approach makes it possible to acquire detailed data on vehicle behaviour at different speeds. The selection of the Vairano track is based on its ability to provide representative data for a comprehensive analysis of longitudinal vehicle dynamics at different speeds. The gradual variation of speeds provides a detailed overview of vehicle behaviour in realistic scenarios. It is expected that the analysis of the data acquired on both tracks will provide an in-depth

\

understanding of the performance of the vehicle's longitudinal dynamics under different driving conditions. This data will form the basis for evaluating vehicle comfort and the performance of the sensors in the vehicle. The post processing has been done in MATLAB environment, after a common resampling function that set the sampling frequency equal to 1 KHz.

\

Chapter 2

Test Description

2.1 The Tracks

As already mentioned, the data analysed in this project came from the measurements from 2 different tracks:

- Ladoux (FR)
- Vairano (IT)

Starting from the French track, is a huge car testing complex owned by Michelin, located in the south of France that offers different tracks depending on the goal's study. The comfort track is 600 meters long (excluding the acceleration line) and it presents different road obstacles, simulating all the possible scenarios of European roads. The used data comes from three different lanes travelled at 50, 80 and 100 kph. The speed of 50 kph has been used in two different lanes called "left lane" and "right lane" and differed in the distribution and geometry of the obstacles. The 80 kph and 100 kph velocities have been used in another lane in order to evaluate the behaviour of the system with different roughness. In fact, this line is divided into multiple sections with two different road roughness level. It should be highlighted that in this test the data coming from the accelerometers were available.

\

Ladoux test track			
Speed	50 kph	80 kph	100 kph
Right Lane	4 measurements	None	None
Left Lane	4 measurements	None	None
Highspeed Lane	None	7 measurements	1 measurement
Vairano test track			
Speed	[15 20 25 30 35 40 45 50 55] kph		
Single Lane	9 Measurements		

Table 1, Data Organisation.

In essence, Michelin's testing complex in the south of France stands as a comprehensive facility, utilizing a sophisticated track layout and diverse testing parameters to comprehensively evaluate noise, comfort, and system behaviour, ultimately contributing to advancements in automotive engineering.

The Comfort Track
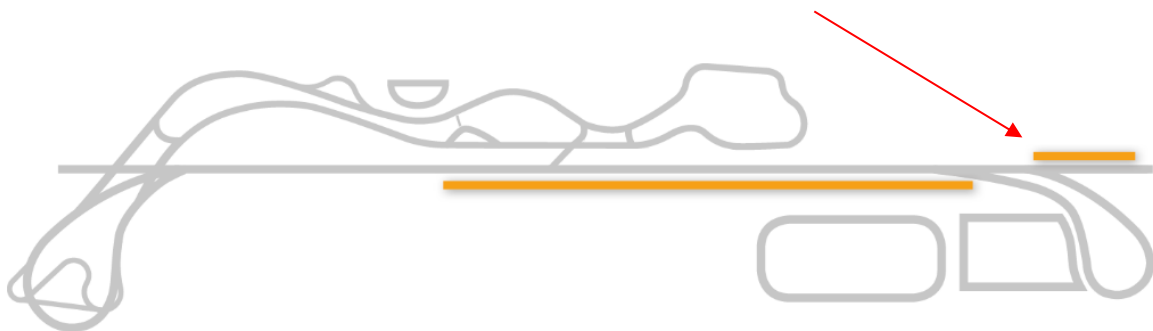
Figure 5, Vairano comfort test track.

The Vairano comfort track is a much smaller testing facility, if compared with the previous one, located in the north of Italy where the car was tested on a single track

\

about 300 metres long and it is used for tests that measure the comfort and handling of cars: noise, creaking, suspension compression and behaviour on road gutters for water drainage.

Figure 6, Type of obstacles on the Vairano test track.

The relevant feature of the data coming from this track is the higher number of different velocities evaluated, in fact, the measurements available cover all the speed between 15 to 55 kph with step increase of 5 kph. This function will be used at the analysis level to understand the behaviour of tires and suspensions as the vehicle speed varies and if it will be possible to identify a particular behaviour of these systems. Unfortunately, in this case only the data coming from the wheel force transducers were available.

\

2.2 Sensor's Description

The most important aspect related to this work relies on the performance of wheel force transducer designed by "Michigan Scientific corporation" that are able to measure forces and momentums in x, y, z directions. The specific model used in both Ladoux and Vairano Test track is the LW12.8-50-TEL, capable of accurately assess the wheel forces and moments acting on both passenger cars and light-duty trucks. The system delivers distinct output signals for vertical, lateral, and longitudinal forces, along with camber, steering, and torque moments. Furthermore, it is designed to withstand various weather conditions, ensuring its suitability for testing in diverse meteorological environments. The telemetry and induction powered electronics are packaged into the transducer to create a low profile and durable assembly. The maximum radial load capacity is equal to 50 kN and the maximum lateral load capacity is equal to 25 kN. Regarding the maximum torque capacity, 6.5 kN·m is the maximum measurable value.
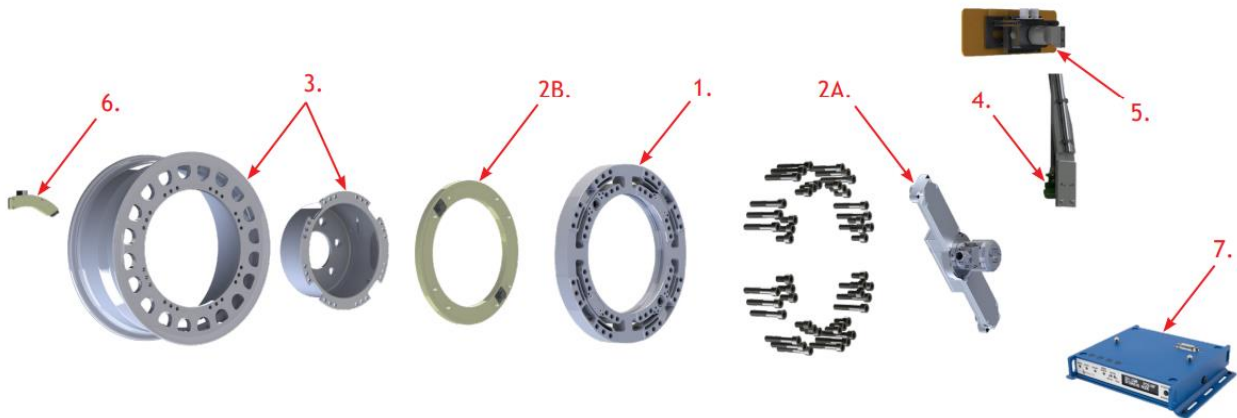
Figure 7, Wheel force transducer assembly.

In the figure above are showed the components of a wheel force transducer:

1. Wheel force transducer

2. Signal Conditioning

   (a) Integrated Slip Ring & Amplifier Subassembly

\

      or

    (b) Wireless Telemetry Transmitter Subassembly

3. Custom hub and wheel adapters

4. Stator restraining rod

5. Stator angle corrector

6. Telemetry stator restraint and bracket

7. CT3 transducer interface box

WFT - Model LW12.8-50		
Maximum force capacity [Fx, Fz]	50	kN
Lateral at Tire Patch [Fy]	25	kN
Maximum Torque Capacity [Mx, My, Mz]	6,5	kN*m
Sensor	4 arm strain gauge bridges	-
Nonlinearity [Fx, Fz, My]	≤ 0.2 % FSO	-
Nonlinearity [Fy]	≤ 0.5 % FSO	-
Nonlinearity [Mx, Mz]	≤ 1.0 % FSO	-
Hysteresis	≤ 1.0 % FSO	-
Sampling frequency	1	kHz
Weight	6.0	kg
Temperature Operating Range	[-40 125]	°C

Table 2, WFT Datasheet.

The other sensors mounted on the vehicle used in Ladoux test track were the accelerometers "PiezoStar" (Type 8766A) fabricated by Kistler. The type 8766 is an IEPE (Integrated Electronics Piezo-Electric) triaxial accelerometer designed for elevated temperature applications. This accelerometer uses Kistler's PiezoStar shear element design which provides wide operating frequency range and extremely low sensitivity to temperature changes.

\

Figure 8, Piezostar accelerometer.

The IEPE sensor combines PiezoStar® crystals and high gain integral hybrid microelectronics to achieve extremely low sensitivity variation over the operating temperature range, compared to other sensing element designs. The Kistler shear element technology also ensures high immunity to base strain errors. The accelerometer uses a welded titanium construction for low mass and an industry standard 4-pin connector for reliable measurements and long-term stability especially at higher operating temperatures. The measurable acceleration range it goes from -50 to 50 g and the measurable acceleration limit it can go up to +/- 100 g.

PiezoStar® Accelerometer - Model 8766A		
Acceleration Range	±50	g
Acceleration Limit	±100	gpk
Sensor	PiezoStar® Sensing element	-
Amplitide non-linearity	≤ ±1.0 % FSO	-
Sampling frequency	1	kHz
Weight	16	g
Temperature Operating Range	[-55 120]	°C

Table 3, Accelerometer Datasheet.

\

Chapter 3

Adopted Procedure

3.1 Track identification

In this dedicated section, an elucidation of the methodological approach employed for the post-processing of data derived from raw measurements is presented. Prior to delving into the comprehensive analysis of data obtained from any kind of automotive track tests, it is imperative to meticulously verify the absence of recurrent errors attributed to human factors. This critical pre-analysis step involves a systematic comparison of data acquired under identical conditions, thereby ensuring the coherence and reliability of the dataset.

Since the starting of measurement, it was decided by a human command, in all the available set of data, it was not consistent to compare data as they were. This judgement was grounded in the recognition that such an approach lacked consistency and could potentially introduce inaccuracies into the subsequent analytical procedures. Consequently, a concerted effort was made to address this initial challenge and enhance the reliability of the subsequent analyses. This involved the meticulous identification of the track profile, a foundational step that underpins the accurate assessment of data consistency and the reliability of measurements.

Furthermore, to ascertain the veracity of the measurements derived from the force transducers at the wheels, it became imperative to establish a robust framework for track profile identification. This intricate process facilitates a nuanced evaluation of the data's consistency, thereby ensuring that the subsequent analytical insights drawn from the force transducers accurately reflect the underlying physical phenomena.

\
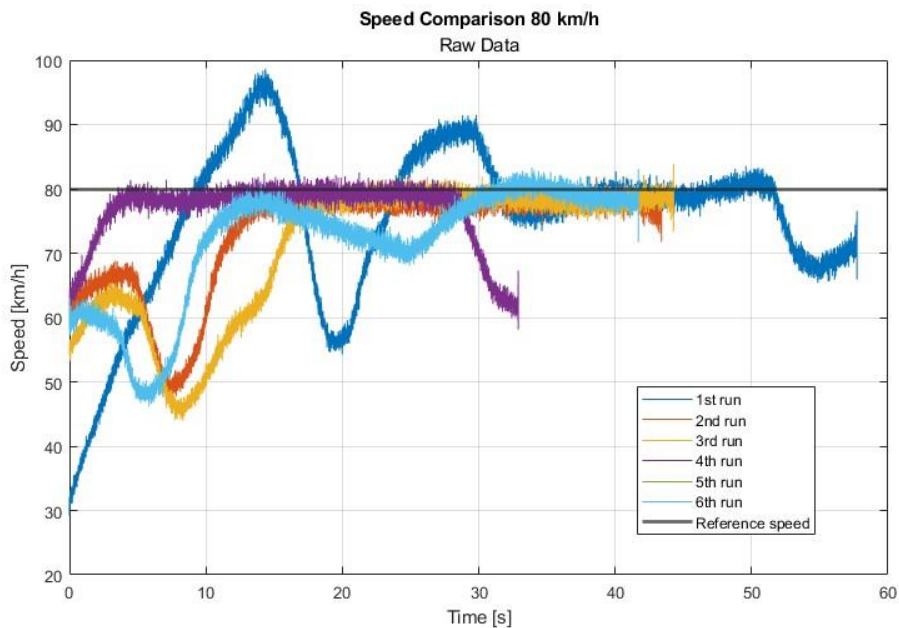
Figure 9, Raw speed comparison.

In essence, the adoption of a systematic and conscientious approach in addressing these considerations are pivotal to the overall integrity and validity of the subsequent data analysis derived from automotive track tests.

The preliminary stage in steering the investigative course involved a meticulous examination aimed at identifying the most effective strategy for the accurate discrimination of data. This effort took into consideration of the foundational insights into the track's intrinsic characteristics, notably its linear trajectory extending over a total length of approximately 300 meters. The decision to leverage this preliminary knowledge was rooted in the recognition that the track's features, characterized by a predominantly straight trajectory, could be harnessed to enhance the precision of data discrimination.

Consequently, a strategic choice was made to employ the latitude and longitude data obtained from the GPS sensor embedded within the vehicle. This decision was underpinned by the understanding that such geospatial coordinates could offer a reliable and comprehensive representation of the vehicle's movement along the track.

\
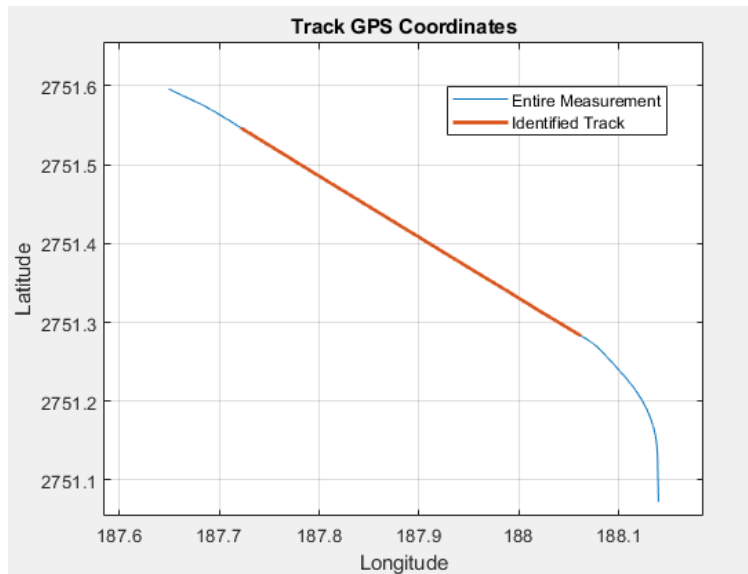
Figure 10, Longitude and Latitude from GPS.

The utilization of these precise location data points provided an effective means to discern and delineate specific segments of interest, particularly during the straightforward trajectory phases of the track. This approach not only aligned with the predetermined knowledge of the track's layout but also constituted a judicious utilization of technological resources to ensure the accuracy and reliability of subsequent data analyses.
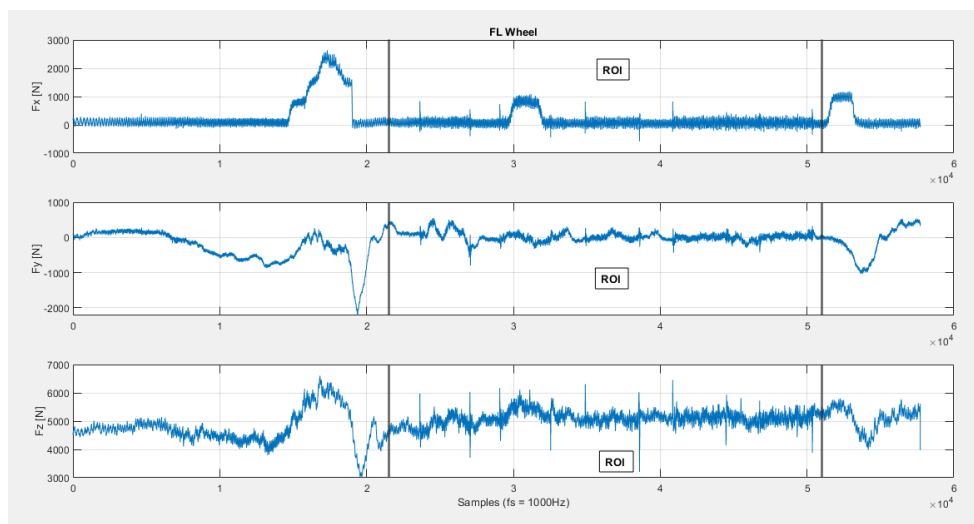
Figure 11, Force in X, Y and Z directions.

\

As it is possible to see from Fig [11], the signals into the highlighted ROI are much more linear, especially the second graph, that shows the evolution of the lateral force over time of the front left wheel, remains close to zero, meaning that the car was not approaching any kind on turn, as expected from this track.
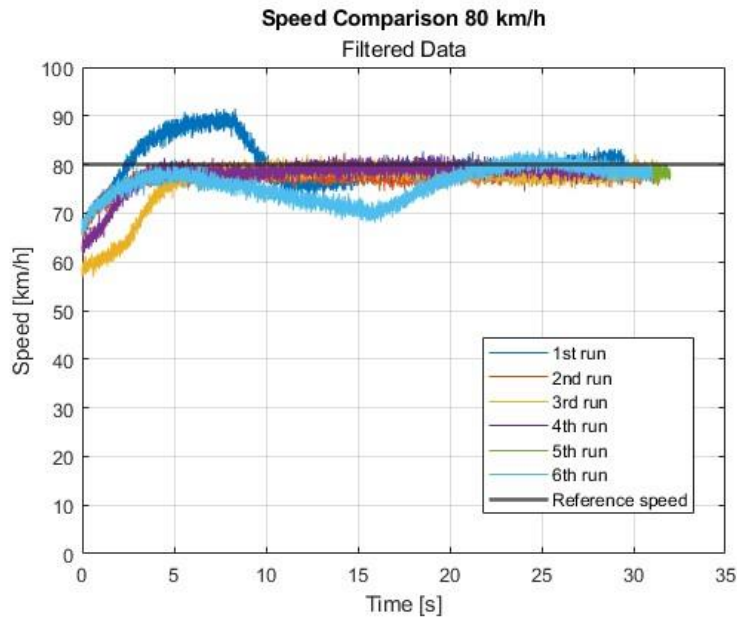
Figure 12, filtered speed comparison.

3.2 Consistency check of data

In the context of data analysis, special emphasis is placed on the importance of data consistency. The robustness and reliability of the information used is crucial for obtaining accurate conclusions and guiding well-informed decisions. Data consistency analysis is an essential step in the process of validation and optimisation of information resources. This step contributes significantly to identifying and correcting any inconsistencies or discrepancies, thus safeguarding the integrity of the decision-making process. Thus, after the identification of the track profile and the right selection of the samples that belong to the region of interest, it was now possible to investigate the data itself and to compare them between data coming from the same lanes, looking for the following features: Completeness, Validity, Consistency and Accuracy.

\

- **<u>Completeness</u>** entails having all necessary data elements present, akin to assembling a puzzle without missing pieces.
- **<u>Validity</u>** ensures data accuracy and conformity to predefined rules and standards, fostering trust in our datasets for meaningful analysis.
- **<u>Consistency</u>** focuses on the uniformity and coherence of data, reducing the risk of errors and ensuring a standardized structure.
- **<u>Accuracy</u>** is paramount for precise measurements and trustworthy calculations, validating data against accepted benchmarks.

Together, these concepts form the bedrock of reliable and high-quality data, supporting informed decision-making and building confidence in the insights derived from thorough analyses. Moving from the theory to the real application, it will be now presented the comparison between all the different track of the French track, highlighting some specific events as examples.
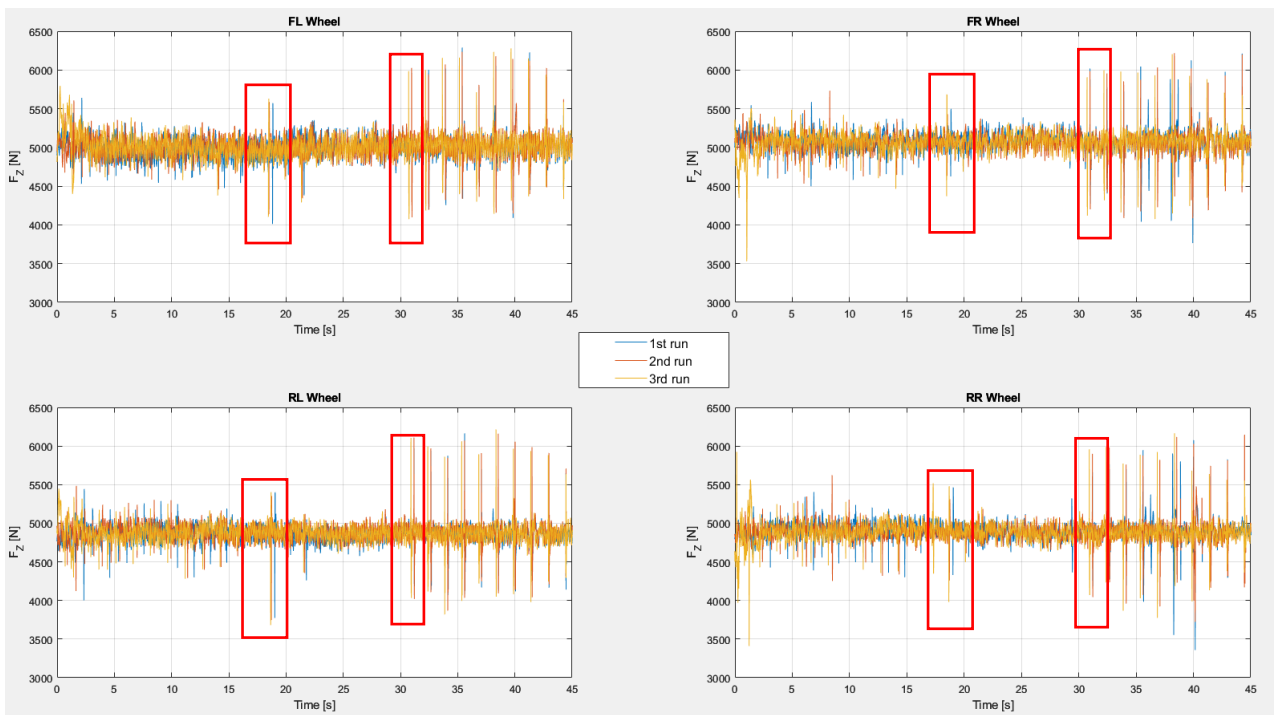
Figure 13, Highlighting events to be analysed.

In the figure above are reported the measured vertical forces from all the four wheels and the red boxes highlight two obstacles on the Left Lane chosen as reference during

\

this process. The motivation on choosing those two events is based on both similar and different characteristics. In fact, in both cases the event is particularly short in time and present a relative high peak if compared with the others time instant and in the other hand the peak magnitude is higher in the second case than the first.

3.3 Time Domain analysis

The examination of individual signals in the time domain includes the independent scrutiny of their time records or the generation of auto-correlation functions. Auto-correlation functions provide a quantitative measure of the correlation between signals and their variations over different time displacements. However, for the purposes of this project, a deliberate decision has been made to abstain from computing the auto-correlation function, as it does not align with the ultimate objectives of this work.

Conducting time-domain observations on an oscilloscope remains an invaluable method, facilitating a direct and comprehensive examination of signal characteristics. This process aids in the meticulous analysis of time histories, enables the identification of signal peaks, and reveals other pertinent features crucial to the understanding of the signal behaviour. Within the realm of good engineering practices, it is imperative to scrutinize the time histories of recorded signals prior to embarking on frequency analysis. This preliminary step ensures a holistic evaluation of signal quality, serving to identify potential issues such as clipping, ascertain signal levels, and detect any peculiarities that may be present within the dataset. This thorough examination establishes a solid foundation for subsequent analyses, especially the analyses in the frequency domain, and enhances the overall reliability of the findings.

\

3.4 Frequency Domain analysis

It is common practice, as it was anticipated in the previous chapter, after completing a time domain analysis moving to a deeper analysis into the system. This happens when a frequency domain analysis it is performed.

Essentially, the frequency domain analysis of continuous signals necessitates transforming the time history of a signal into an auto-spectral density function. This transformation is achieved through a Fourier transformation of the auto-correlation function.

The Fourier transform is:

$$F(\omega) = \int_{-\infty}^{+\infty} f(t)\, e^{-j\omega t}\, dt$$

The Fourier Transform is a mathematical technique that decomposes a signal, typically a function of time, into its constituent frequencies. Named after the French mathematician Jean-Baptiste Joseph Fourier, the transform allows us to analyse the frequency content of a signal by expressing it as a sum of sine and cosine functions. The Fourier Transform is particularly useful in various fields, including signal processing, communications, and image analysis.

In short, the Fourier Transform takes a time-domain signal and converts it into its frequency-domain representation. This transformation provides valuable insights into the different frequency components present in the original signal, helping analysts and engineers better understand its characteristics and behaviour. The inverse Fourier Transform can also be applied to reconstruct the original signal from its frequency components. Overall, the Fourier Transform is a fundamental tool in the study and manipulation of signals in both time and frequency domains.

\

In practice, digital fast Fourier transform (FFT) techniques are utilised and, also in this project, the mathematical software MATLAB has performed this transformation.

In this work, the main functions of the frequency domain were used to perform an accurate analysis. the functions are:

- Power Spectral Density (PSD)
- Cross - Power Spectral Density (C - PSD)
- Magnitude Squared Coherence (MSC)

These functions can be divided into two different types of analysis, because the PSD measures the distribution of power or energy in a single signal as a function of frequency it belongs to an "individual signal" analysis function. Meanwhile, The C – PSD and the MSC need two signals because, the first one computes the distribution of power or energy between two different signals as a function of frequency and it provides insights into the relationship between the frequency components of two signals and how their power varies with respect to each other. The MSC provides information about the strength and consistency of the relationship between the frequency components of two signals. Because of that these functions belong to the "Dual signal" analysis.

\

Chapter 4

Time Domain analysis

4.1 Consistency

As already explained in the previous chapters, the first step of the analysis was focused on the comparison of all the available measurements coming from all the investigated tracks. In the following paragraphs, the data of the three French runways and the Italian runway in Vairano will be illustrated.

4.1.1 Left Track at Ladoux
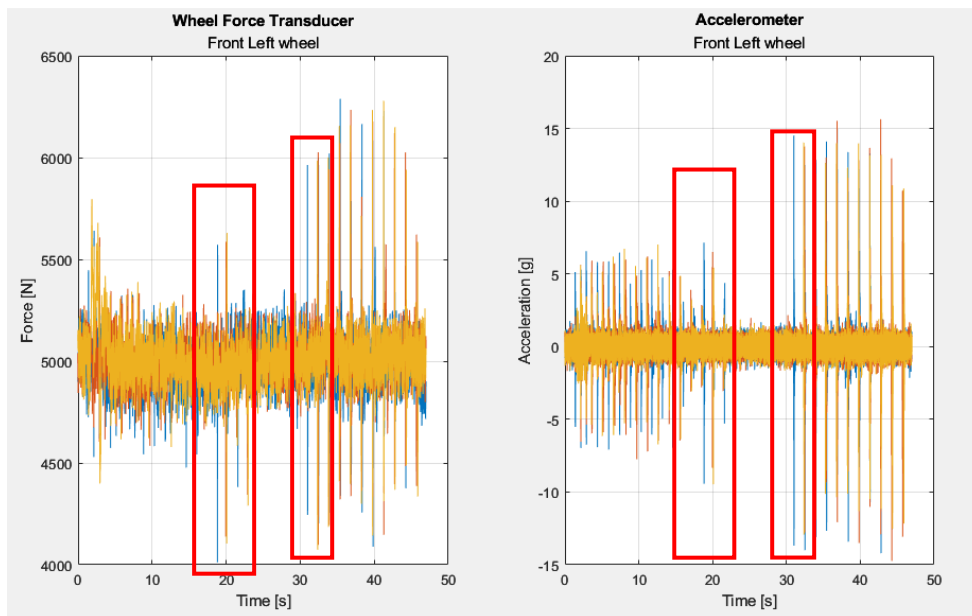

Figure 14, Events analysis for Left track low speed.

The first tracks to be analysed is the left lane of the slower part of the circuit, travelled at 50 km/h three times, the peculiarity of that specific track is that there is no difference

\

between the obstacles placed to excite the two wheels, so excitation is symmetrical for the left and right side of the vehicle. As it would be too time-consuming to analyse all the points collected by the sensors individually, it was decided to concentrate the analysis on two distinct and clearly recognisable events, highlighted by the Fig. [14].

In the figure below is reported the first zoom on the front left wheel for the three runs on this track.
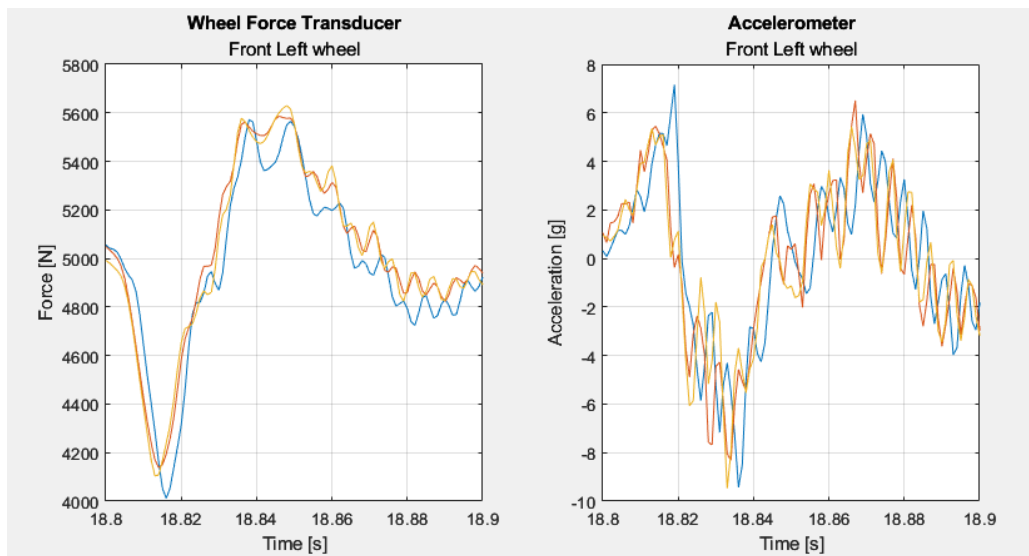
Figure 15, Zoom on the first event.

As illustrated in Fig. [15], a detailed examination of both cases reveals notable similarities in their respective measurements. Focusing on the WFT scenario, it becomes evident that the signals exhibit a remarkable degree of resemblance. Following a meticulous adjustment to align them perfectly, the peaks in the signals virtually mirror each other, indicating an almost identical profile. Notably, the sensor excels in capturing the characteristic double oscillation that is consistently highlighted in theoretical analyses when a vehicle model encounters a cleat.

In the second case, when considering the accelerometers, a commendable level of consistency akin to the previous sensor is observed. Despite this commendable consistency, a discernible distinction arises in the nature of the outputs. While they remain comparably aligned, the signals from the accelerometers appear more

\

susceptible to the influence of external disturbances. These disturbances introduce a certain level of corruption, overshadowing and, in fact, completely concealing the double oscillation that is conspicuously visible in the first case. This divergence in signal quality raises intriguing questions about the susceptibility of different sensors to external factors and underscores the importance of understanding and mitigating such influences in experimental measurements.
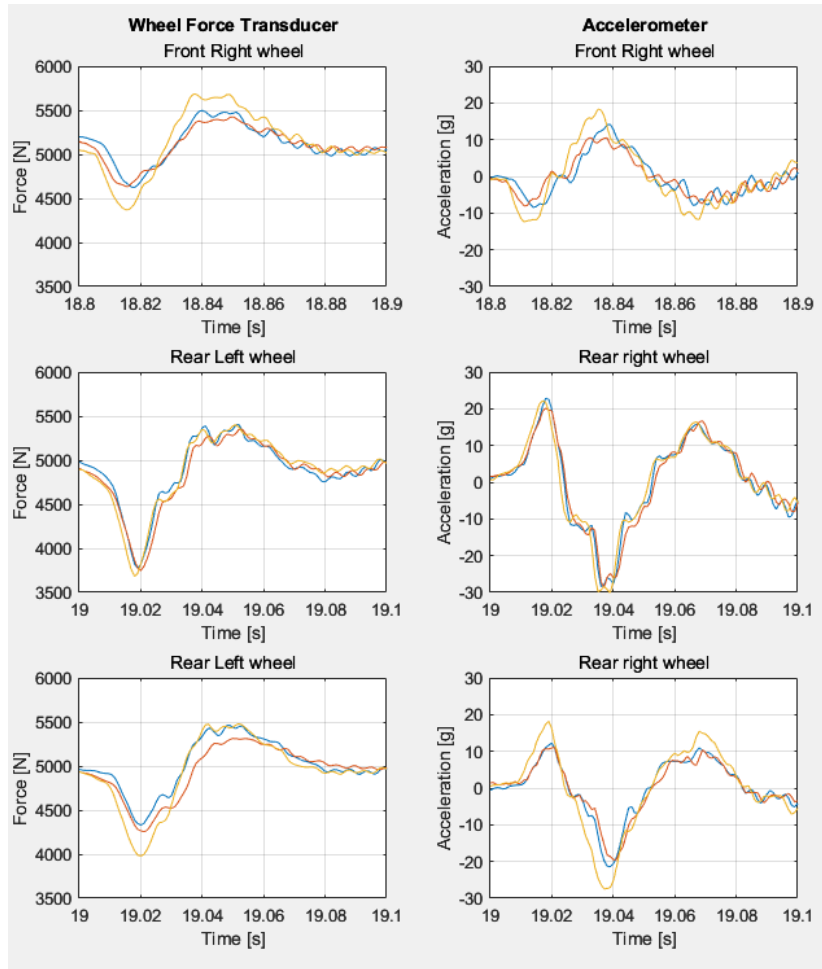
Figure 16, Second zoom for the other wheels.

From the picture above it is possible to understand that the performance examined in the first part of the paragraph are valid also for the other sensors. It should be noted that, contrary to what it has been shown before, the accelerometers mounted on the other wheel hubs are not showing the more corrupted behaviour. In the end, the

\

performance of the sensors is comparable, with a better capability of the WFT on capturing the intrinsic dynamic of the event. It is visible especially in the Fig. [15].
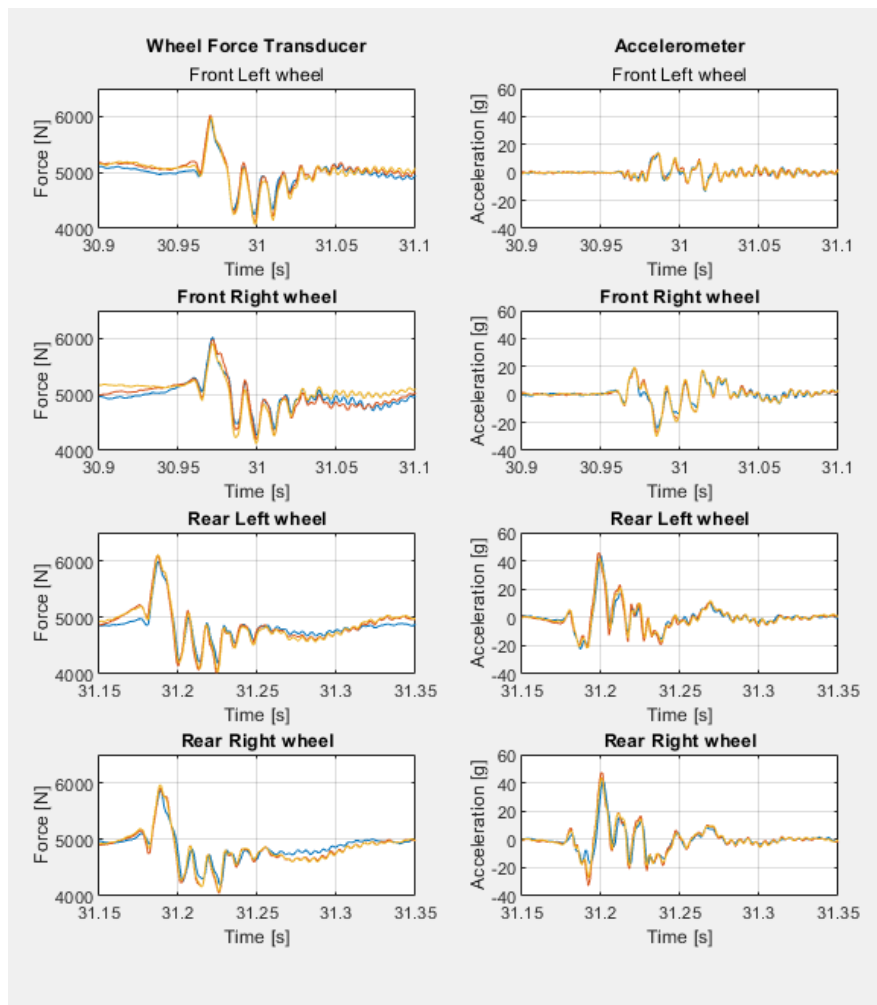
Figure 17, Zoom on the second event.

The Fig. [17] shows the measured signal from the other chosen event, as expected from the previous analysis also in this case the consistency is considerably high, confirming the high quality of measurements. It should be noted that the excitation lasts in both the WFTs and the accelerometers for higher time, keep oscillating the suspensions more than the previous case.

\

"Left" Track		
Features		
Speed	50	km/h
Sampling Frequency for both sensors	1	kHz
Measured Signals		
WFT		Force [Fx, Fy, Fz]
Accelerometer		Acceleration [Ax, Ay, Az]

Table 4, Data Recap for the "Left" Track.

4.1.2 Right Track at Ladoux
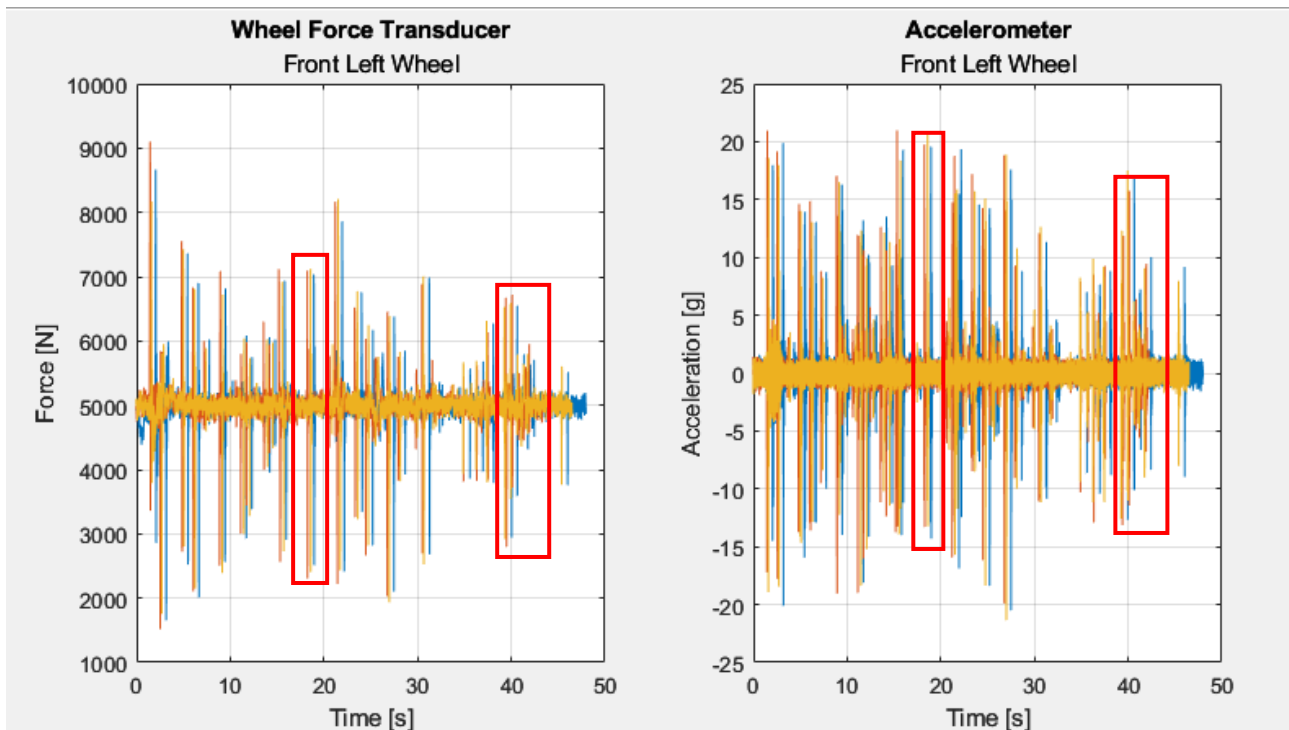
Figure 18, Events analysis for Right track low speed.

This paragraph delves into the detailed description of the second track, specifically the right lane, which was traversed at a speed of 50 km/h. A notable distinction from the previous scenario becomes apparent when considering both the distribution of obstacles and the magnitude of excitation. In contrast to the left lane, the right lane exhibits a distinct arrangement of obstacles, contributing to a completely different dynamic response.

\

One key observation lies in the peak force recorded by the WFT during this run, reaching approximately 9000 N. This marked increase in force stands in stark contrast to the peak force measured on the left lane, which was recorded at around 6000 N. This variance in excitation magnitude emphasizes the dynamic nature of the two tracks, with the right lane presenting a more demanding and forceful environment.

Extending this analysis to the accelerometers on the right lane, a parallel distinction emerges. The data from these sensors further supports the previously observed trend. While maintaining commendable consistency comparable to the left lane, the accelerometers on the right lane record signals that reflect the heightened influence of external factors. This amplification is manifested in the higher excitation magnitude, underscoring the significance of considering individual track characteristics in comprehensive experimental assessments.

The procedure used in the previous chapter to analyse the consistency of the measured data is reused here, again considering the dynamic response of the two events highlighted in Fig. [18]. In the figure below is reported the first zoom on the front left wheel for the three runs on this track.
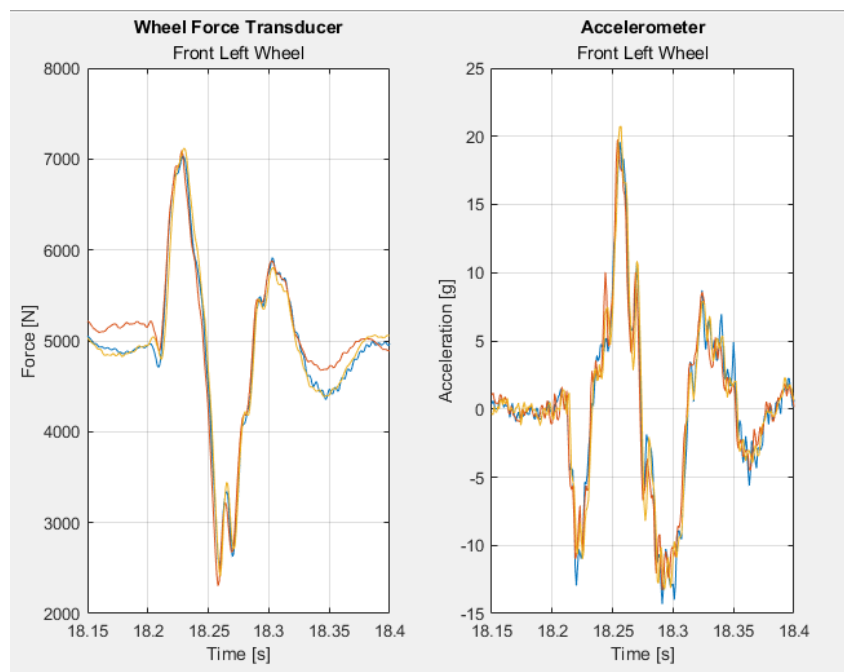
Figure 19, Zoom on the first event.

\

As might be expected, there are no macroscopic differences between the measured runs, on the contrary, the data are perfectly aligned, once again confirming the robustness of these tests. It must be underlined that even in this case the behaviour mounted on the front left wheel hub shows a more jagged characteristic. From the figure [#sopra] it is also clear how different the severity of the obstacles encountered is between the two tracks, this can be seen both from the force and acceleration peaks measured and from the time it takes for the system to absorb the vertical excitation. in fact, the time taken to overtake the obstacle in the left track was about 0.1 s, whereas in this second case it is almost twice as long.
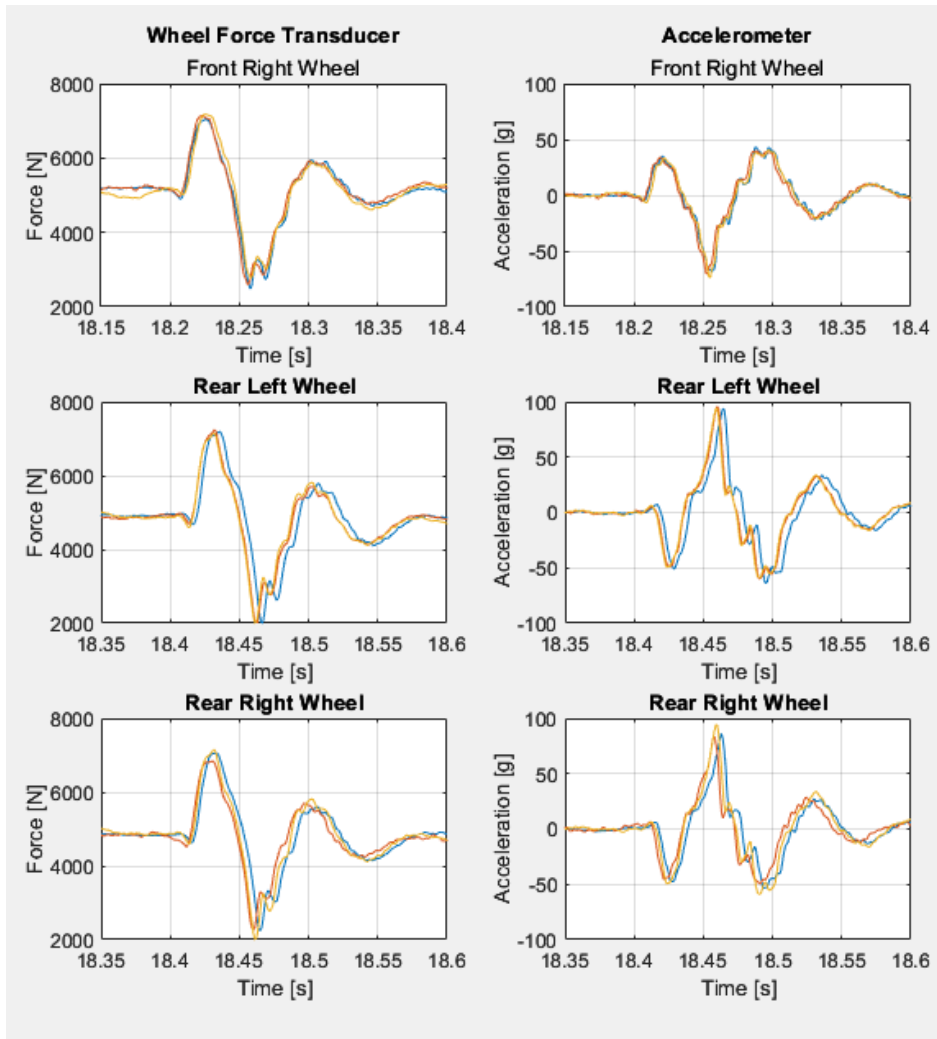
Figure 20, Second zoom for the other wheels.

\

The image above provides insights into the performance evaluated in the initial portion of the paragraph, indicating that the observed characteristics are applicable to the remaining sensors as well. Al already explained in the paragraph 4.1.1, the sensors exhibit comparable performance, with the WFT demonstrating a superior ability to capture the intrinsic dynamics of the event. This distinction is particularly evident in the accompanying figures.
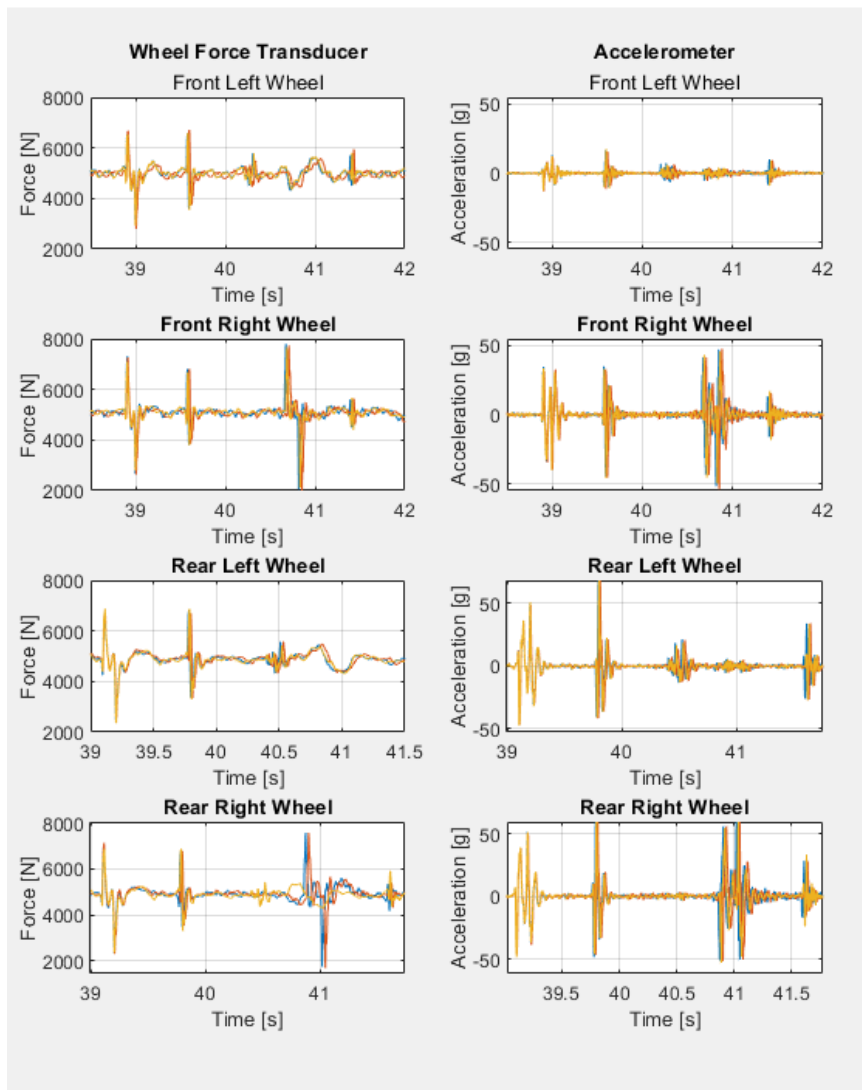
Figure 21, Zoom on the second event.

Furthermore, regarding the second zoom of the right track, it has been decided to increase the time length of the analysis in order to investigate a more general behaviour

\

of the vehicle itself and especially the ability of the sensors to capture the input coming from the road correctly. In the Fig. [21] it immediately stands out the unexpected discrepancies in terms of magnitude between the Front Left wheel signal measured by the accelerometer and the others not seen in the previous cases. This could be explained or with an error of the driver that during the measurement was not able to keep the car perfectly aligned with the track, "missing" with the front left wheel the optimal contact point with the obstacle. It would appear that the same thing has also happened in the Rear right case measured by the WFT, where the yellow line fails to capture the excitation coming from the road, as present in the other two cases. Moreover, from this last figure, it can be seen the differences on obstacle distribution between the right side and the left side.

"Right" Track		
Features		
Speed	50	km/h
Sampling Frequency for both sensors	1	kHz
Measured Signals		
WFT	Force [Fx, Fy, Fz]	
Accelerometer	Acceleration [Ax, Ay, Az]	

Table 5, Data Recap for the "Right" Track.

4.1.3 Highspeed track at Ladoux

In this paragraph it will be presented and described the last track of the Ladoux facility, travelled at 80 and 100 km/h. The peculiarity of this case is that there are not "concentrated" obstacles but there are two alternating levels of roughness as shows Fig. [22]. The alternating roughness is much more visible on the accelerometer side due to its capability to measure very fast vibrations. In this case, due to higher density of data, it has been decided to present just one case and, since the consistency it has been already demonstrated on the previous cases and the test have been run in the same day and with the same configuration, it was not considered to check it again, keeping

\

as result the same observations done before. This approach ensures efficiency in data analysis while maintaining confidence in the overall findings.
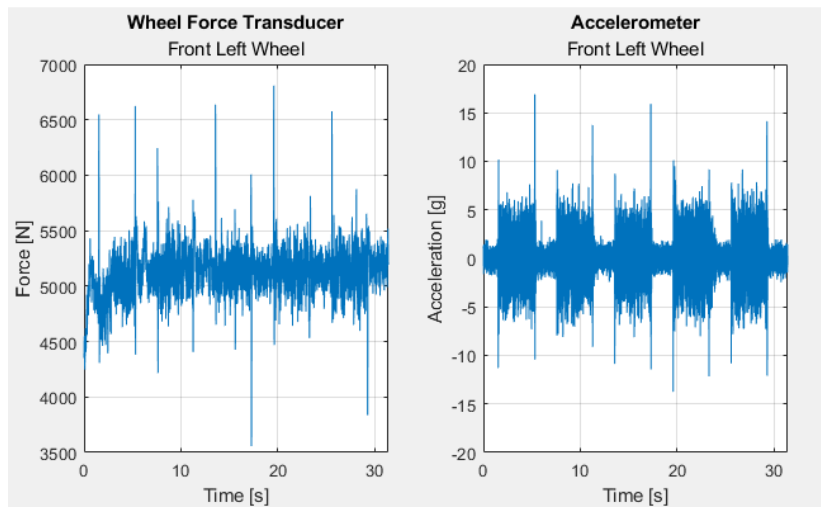
Figure 22, Highspeed track measurements.

For the sake of completeness in presenting the data, Fig. [23] presents the measurements made for the other three wheels.
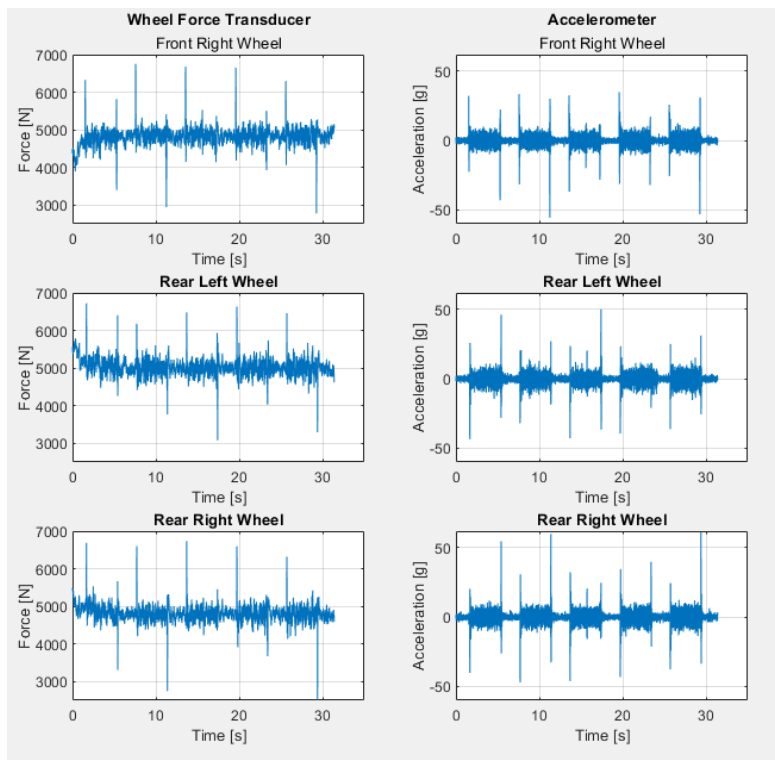
Figure 23, Measurements from the other wheels.

\

"Highspeed" Track		
Features		
Speed	80, 100	km/h
Sampling Frequency for both sensors	1	kHz
Measured Signals		
WFT		Force [Fx, Fy, Fz]
Accelerometer		Acceleration [Ax, Ay, Az]

Table 6, Data Recap for the "Highspeed" Track.

4.2 Vairano test track: Time Domain and Space Domain

This section is dedicated to present the measured data on the Vairano's test track. It should be remembered that the accelerometers were not mounted on the vehicle and the next analysis are based solely on data coming from WFTs. Compared with the other analysed track, the obstacles coming from the road were not easily identifiable and there were more than one road surfaces to be travelled as it can be seen from Fig. [6]. Moreover, as it is possible to see from Fig. [24], since the same track was travelled at different velocities, the duration of the measurements was obviously different.
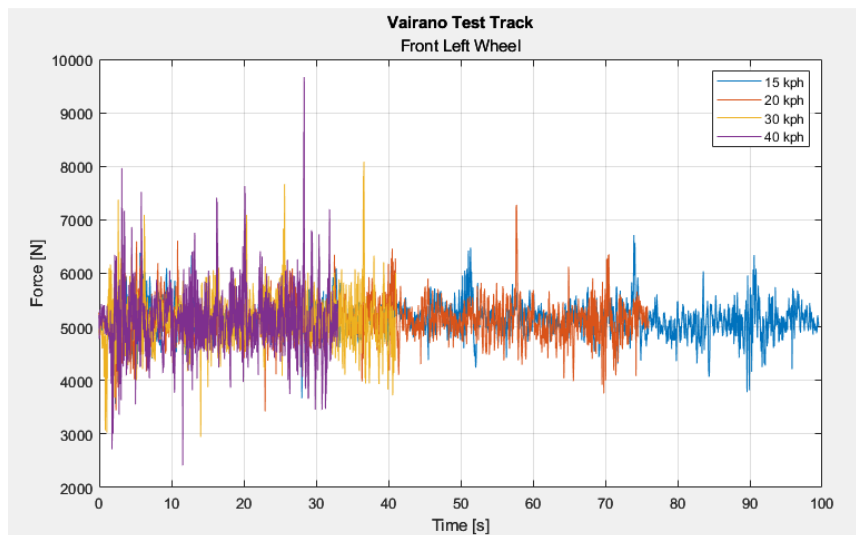
Figure 24, Different measurements of the Vairano test track.

\

To facilitate data comparison, a shift from the previously examined time domain to the spatial domain has been chosen, leveraging the straightforward correlation between speed, space, and time. This methodology finds extensive application in the automotive sector, particularly in motorsports, as it enables the consistent comparison of measurements at identical locations, such as turns or chicanes, from one lap to the next. This approach helps mitigate discrepancies arising from minor speed fluctuations, enhancing the accuracy of performance assessments. From figure [sotto] it can be seen that the data look quite different from Fig. [24] and, luckily, much more
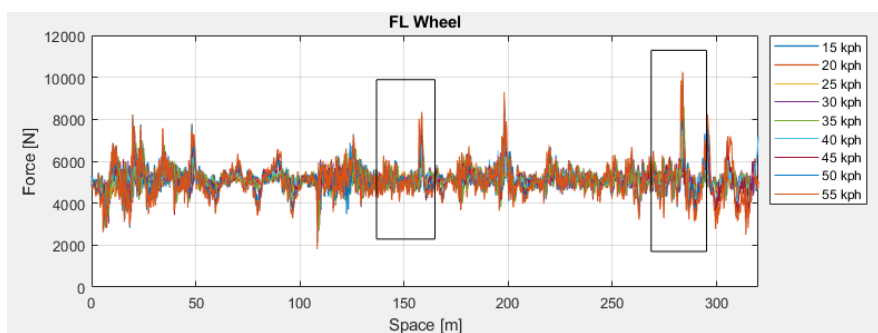
Figure 25, Chosen event to be compared.

comparable. Moreover, as a further confirmation of the process, the calculated travelled distance complies with the length declared by the ownership of the test track. Thus, the aim of this section is, therefore, to search for peculiarities in the behaviour of the vehicle when it is excited at different speeds by the same obstacle on the track. Two rectangles can be seen in Fig. [25] which highlight the sections of the track chosen to make this comparison.

\
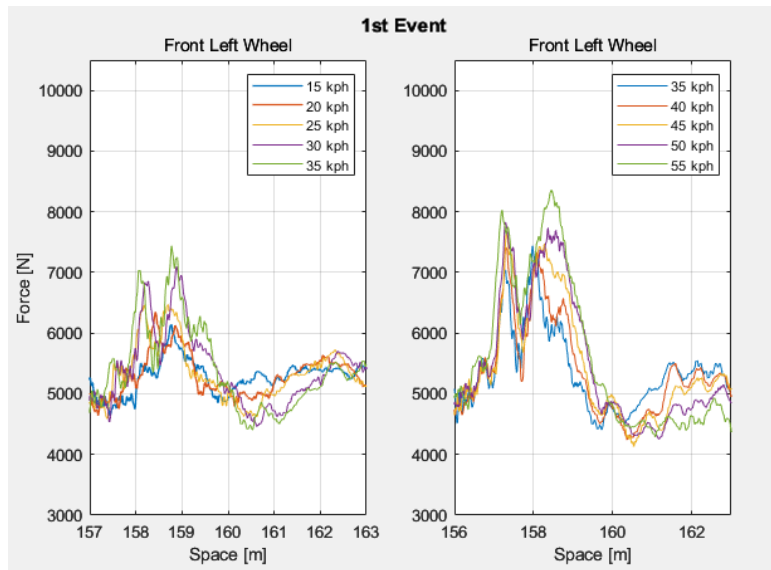
Figure 26, Zoom on the first event.

The data measured from the front left WFT are depicted in Fig. [26], for the sake of clearness the measurement coming from different run has been divided into two different graphs. As it can be observed, there lacks a discernible threshold speed at which the tire-suspension system exhibits an anomalous surge in force attributable to road excitations. Conversely, the recorded vertical force demonstrates a gradual increment with escalating speeds, aligning with the anticipated behaviour in such scenarios. Notably, this characteristic is not confined to the front left WFT alone but resonates across all four wheels of the instrumented vehicle, establishing a consistent trend in the observed phenomena. Below are depicted the measurements coming from the other wheels. This behaviour reflects the absence of critical frequency in which the suspension system is not able to filter and to damp the input coming from the road, ensuring high levels of comfort inside the vehicle.

\
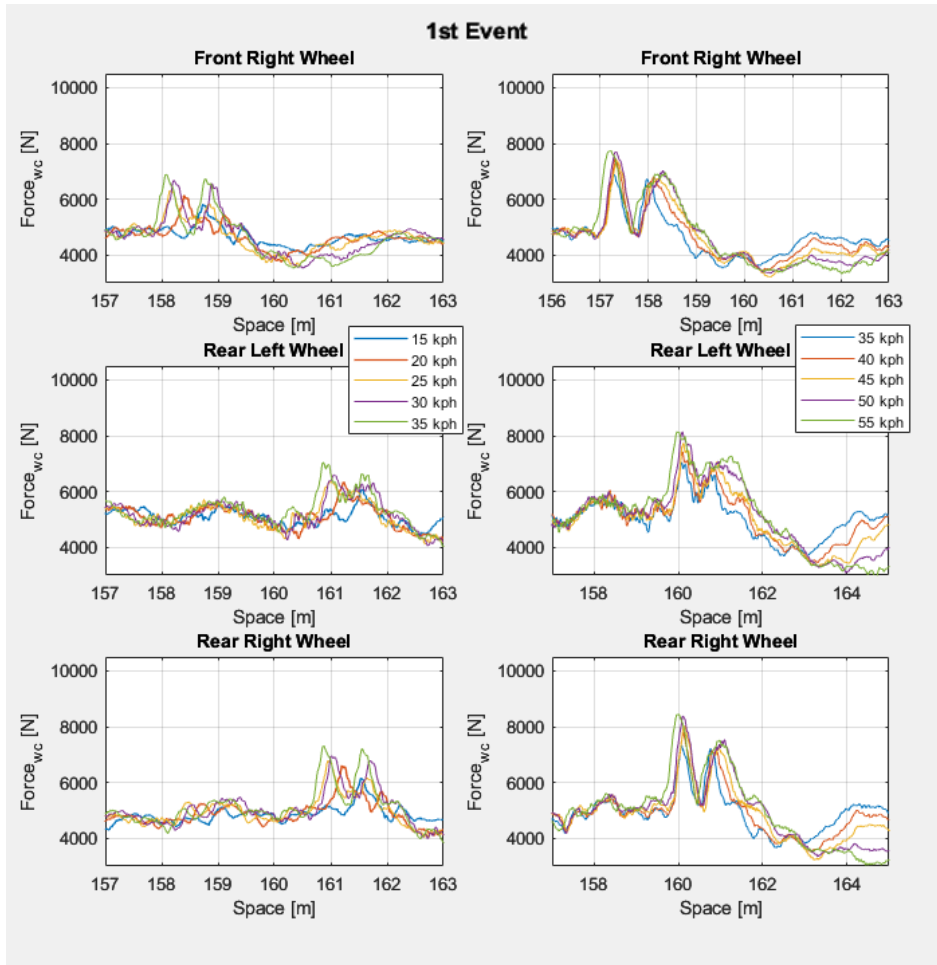
Figure 27, Measurements from the other wheels.

As further confirmation of the assessments made for the first case, a second event, relatively distant from the first, was also analysed. Compared to the first one, the measured peak force is certainly greater, and in addition the vehicle, before encountering this obstacle, has faced a series of holes, thus already being dynamically disrupted.

\
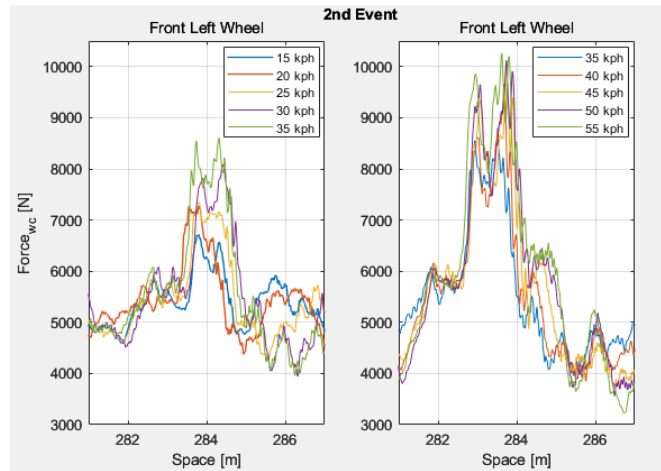
Figure 28, Zoom on the second event.

As consistency with the other measurements had already been shown above, only the results from the left front wheel are shown. As already mentioned, the absolute variation of the forces is much greater than in the first case, despite this the general behaviour remains unchanged, there are no unexpected peaks, and the measured force increases with increasing speed. This confirms the ability of the suspension to correctly damp the excitations coming from the road.

This analysis did not reveal any unexpected behaviour of the wheel-suspension system. Unfortunately, due to the lack of acceleration sensors, it was not possible to investigate further and make a comparison with the dynamometric wheels.

\

Chapter 5

Frequency Domain analysis technique

Following the comprehensive examination conducted in the preceding chapter, the assessment of data transitions to the frequency domain. A crucial aspect of frequency-domain analysis is its ability to illustrate how the energy of a signal is distributed across various frequencies. Whenever a signal can be depicted through amplitude variations over time, it possesses a corresponding frequency spectrum. This spectrum precisely signifies the portrayal of a time-domain signal in the frequency domain. Numerous physical signals can be decomposed into the summation of elementary signals at distinct frequencies. The objective of frequency domain analysis is to ascertain information such as amplitude, phase, power, etc., for a signal at different frequencies.

Figure 29, Frequency domain analysis features.

As shown in Fig. [29], time domain analysis and frequency domain analysis offer distinct perspectives for examining a signal. Typically, time domain analysis is

\

considered the more intuitive approach, particularly when dealing with straightforward periodic signals. The analysis in the time domain provides a direct insight into the signal's amplitude variations over time. However, its limitation lies in its capacity to reveal the frequency composition of the signal.
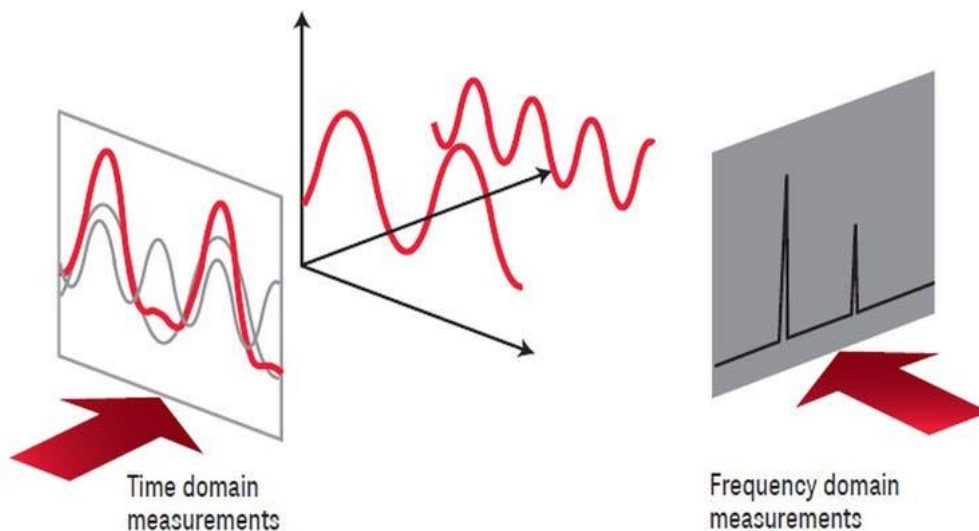
On the contrary, the frequency spectrum employs frequency as the horizontal axis and the amplitude of each frequency as the vertical axis, providing a graphical representation that effectively communicates the frequency composition of the measured signal. While waveform analysis primarily captures changes in signal amplitude over time, it often falls short in providing a clear visualization of the signal's frequency composition. In this context, the frequency spectrum emerges as a valuable tool, offering a direct and informative display of the signal's frequency components. There are several advantages to perform this type of analysis:

1. Frequency domain analysis has a clear physical meaning. When physical phenomena such as visible light, music, radio waves and vibration are analysed in frequency domain, the cause of the signal and its related information can be explored.

2. Complex signal analysis. Simple sinusoids are easier to identify from the waveform, but the time domain waveforms for signals involving multiple harmonics. Whereas, for the complex signals with multiple frequencies, their frequency components are difficult to be found in time domain while easy to be seen in frequency domain.

3. Strong anti-noise ability. Actual signals usually contain noises. In the time domain, the signal is not smooth and has lots of spikes. It increases the difficulty of information identification. In the frequency domain, the noise is usually weak and easy to be separated, and main components in signal are easy to be highlighted.

\

5.1 PSD

The power spectral density (PSD) serves as a crucial analytical tool, based on the Fast Fourier Transform, in signal processing and engineering, offering a comprehensive insight into the frequency characteristics of a signal. In essence, the PSD unveils the distribution of power across different frequencies, unravelling the intricate nuances that define the behaviour of a system. By delving into the spectral domain, it is possible to obtain a great deal of information on the frequency components of a signal, providing a basis for in-depth analysis. As can be read in many papers [2] [7] [8] [9], PSD is commonly used in the automotive sector for a wide variety of applications, including comfort analysis. The PSD has been calculated thought MATLAB with the function "pspectrum" that refers to:

$$S(f) = lim_{T \to \infty} | \int_{0}^{\infty} x(t)e^{-j2\pi ft} dt|^2$$

Where:

- S(f) is the PSD
- x(t) is the time domain signal
- f is the frequency

Before proceeding with the presentation of data, it is important to specify the cut-off frequency equivalent to the Nyquist frequency, which, by definition, is half the sampling frequency and indicates the maximum frequency an analogue signal can have before it can still be correctly converted into a digital signal. The WFT's sampling frequency was 1 kHz. Thus, the limiting frequency used to calculate the PSD (and the other functions in the frequency domain) is 500 Hz.

Since the consistency of Data has been already proved in Chapter 4, in the next pages the evaluation will be presented for just the front left wheel force transducer and accelerometer. The first track to be presented is the low-speed track named "right". The

\

calculated PSD is plotted in double logarithmic scale, useful when dealing with functions that have a wide range of magnitudes, as it allows you to visualize both small and large values on the same plot.
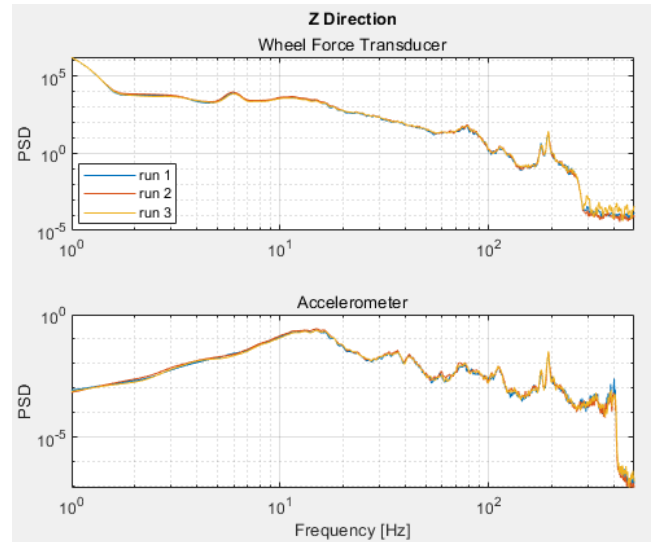
Figure 30, Front Left wheel PSD, Right track.

Fig. [30] shows the PSD coming from the measurement of the WFT and the accelerometer. Clearly, the order of magnitude on the y axis is completely different due to the intrinsic difference of the two signals, as they measure two different quantities. Beyond that, the power distribution over the frequency spectrum results different, especially at low frequencies. In fact, the first difference is the existence of a slight hump around 5 Hz in the WFT graph, this hump being completely absent in the accelerometer measurement. Moreover, the accelerometer's PSD continuously increases up to create a peak slight after 10 Hz. This slight increase of power content at that specific frequency it has not be detected by the WFT. Then, around 100 Hz the behaviour of the two curves remains comparable, highlighting an important peak around 200 Hz, Perry Gu et al [10] have found that air cavity resonance phenomena show peaks in the frequency range around 200 Hz. More detailed analysis, especially with specific laboratory's tools, should be carried out in order to confirm that also in this study.

\

Moving on with the presentation of the data obtained, the next track is the one, again at low speed, called "left".
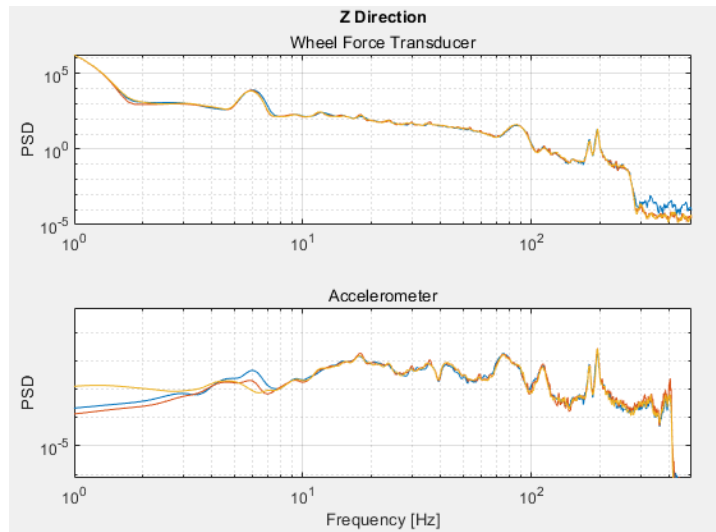

Figure 31, Front Left wheel PSD, Left track.

Also in this case, the general behaviour is consistent with the one presented above. In contrast to the "right" track, the energy peak around 5 Hz is greater and this time the accelerometer seems to detect this increase in energy content, which was not previously visible.
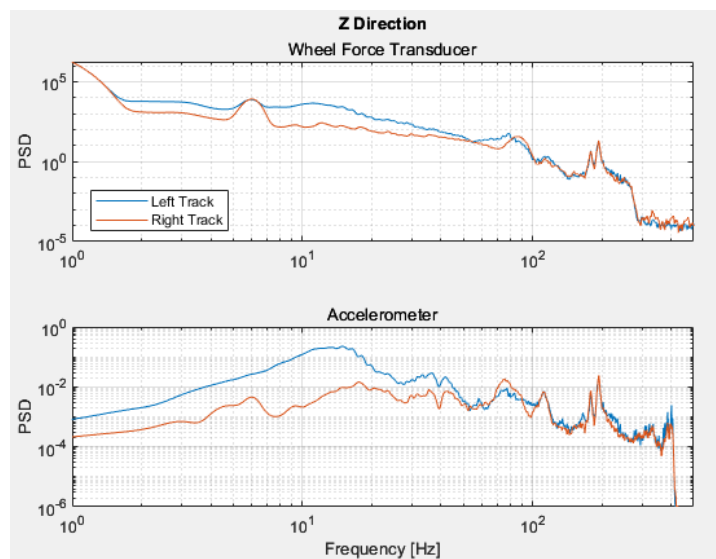

Figure 32, Comparison of the PSD for the two low-speed tracks.

\

Fig. [32] presents the differences between the two tracks in the calculation of PSD in an easier-to-view manner. As we move on with the presentation of the data, it will now be presented the data from the high-speed track, in this case it was decided to simultaneously analyse the data at 80 km/h and those at 100 km/h as the track is the same. As explained in chapter three, in this case the high-speed track does not have bumps but road sections with different roughness.
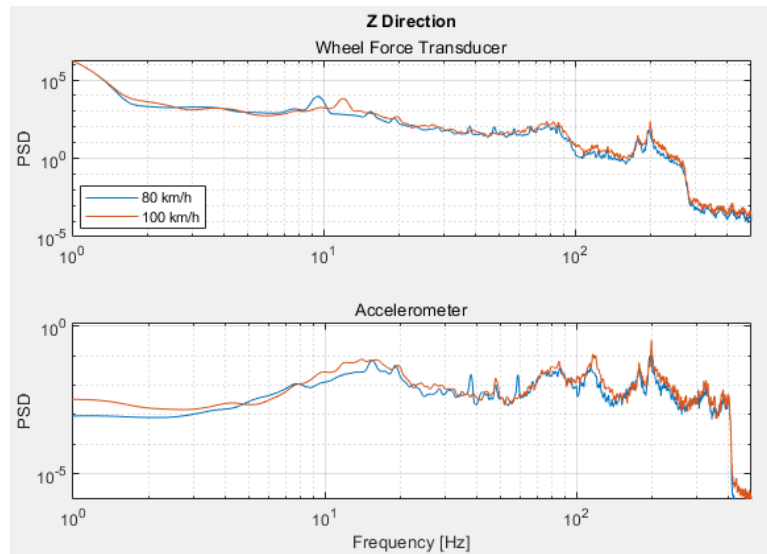
Figure 33, PSD of the highspeed track at two different velocities.

In the overall picture, the observed behaviour consistently mirrors that recorded in the two preceding scenarios. Notably, the dominant peaks at 200 Hz persist and are unmistakably evident in this instance as well. However, a notable and unexpected occurrence surfaces, a distinctive peak, exclusively identified in Wheel Force Transducer (WFT) measurements, emerges around 10 Hz. Intriguingly, this particular peak appears to exhibit a frequency shift towards higher values as speed undergoes variations. To delve deeper into the intricacies of this unexpected peak, comprehensive insights are garnered by juxtaposing measurements from all three tracks. The ensuing analysis, illustrated in Figure [], underscores the significance of considering diverse speeds in elucidating the characteristics of this peculiar frequency phenomenon specifically observed in the context of Wheel Force Transducer data. Thus, observing the 4 measurements shown in the figure below, there is a further confirmation of the

\

shift of the peak highlighted above according to the speed of the runway. in fact, at 50 km/h the peak moves to lower frequencies. In addition, data from all four wheels were plotted for completeness, and this phenomenon is present in all four cases.
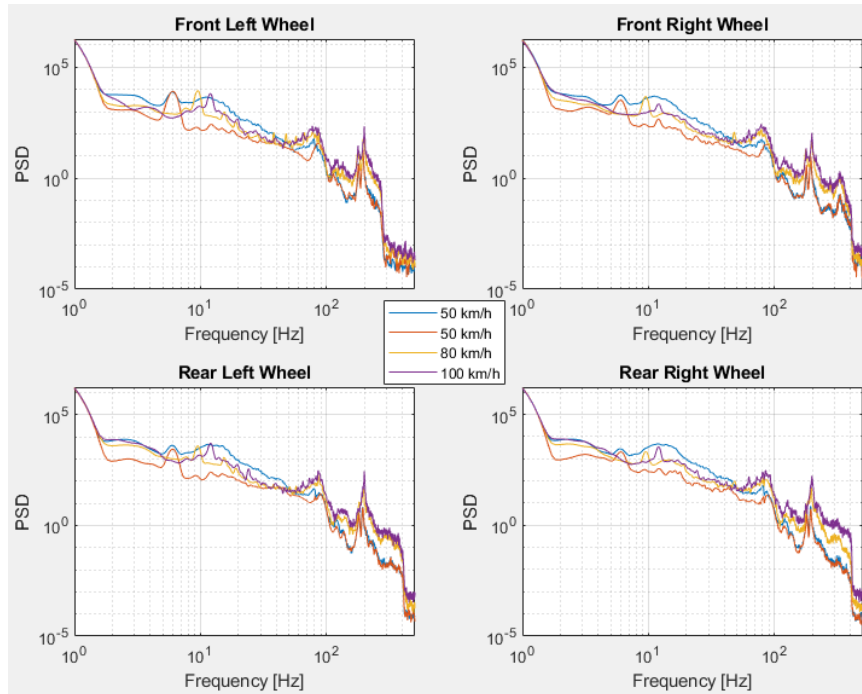
Figure 34, Highspeed PSD of all the wheels.

One of the first explanations tried to give to this phenomenon concerns a possible imperfection in the WFT mounting that could cause an overall imbalance at the wheels level, which would explain the peak movement, which would vary with the frequency of tyre rotation, since the WFT is mounted on the rim. Thus, in order to pursue this hypothesis, the rotational frequency of the various cases has been calculated. From the data given by the manufacturer the wheel radius is equal to 0,36 m. The used formula to calculate the frequency is: $f = \dfrac{V}{3.6 \cdot R \cdot 2\pi}$

\

Nominal speed	[Km/h]	50	80	100
Real speed (mean)	[Km/h]	48,92	80,16	96,87
Calculated frequency	[Hz]	6,00	9,84	11,89
Peak	[Hz]	5,98	9,52	11,97

Table 7, Rotational frequency vs PSD peaks.

Summarizing what can be seen from the table above, it becomes apparent that the hypothesis is seemingly affirmed, given the closely aligned trends between the calculated values and those observed in the graphical measurements. However, it is imperative to acknowledge the inherent limitations and the unfulfilled potential for further confirmation or refutation of this hypothesis. Unfortunately, the constraints imposed by the test themselves render it challenging to conduct additional research. Specifically, the inability to have more data with different features, such as vary the speed or implement dedicated measurement runs where force transducers could be meticulously controlled and potentially aligned with the wheels hampers the exhaustive exploration of alternative scenarios. Consequently, while the existing data suggests a positive correlation, it also underscores the need for caution in drawing definitive conclusions, emphasizing the importance of future research endeavours with an expanded scope of experimental possibilities.

5.2 Cross Spectral Density

The Cross spectral density belongs to the so-called dual signal analysis techniques of the frequency domain. The cross-spectral density is a complex function, it is the Fourier transform of the cross-correlation function. It is a measure of the mutual power between two signals, and it contains both magnitude and phase information.

\

$$S_{xy}(f) = \int_{-\infty}^{+\infty} \left[\lim_{T \to \infty} \frac{1}{T} \int_{-\infty}^{+\infty} x_T^*(t-\tau) \cdot y_t(t)dt \right] e^{-i2\pi f\tau} d\tau = \int_{-\infty}^{+\infty} R_{xy}(\tau)e^{-i2\pi f\tau} d\tau$$

Where x and y represent the two studied signals.

It could involve relationships between two input signals to a system, or two output signals from a system, or an input and an output signal. In the case-study analysed in this thesis the two signals used to compute the Cross spectral density are an input and an output of the suspension system. In this specific function, MATLAB calls up the function with the command 'cpsd', which, in addition to the sensor sampling rate, requires other information to be provided as input. Which are:

- Sampling frequency = 1 kHz
- Window (number of samples taken every calculation) = 450
- Hamming's window (Default value)
- Noverlap (number of overlapping samples) = 45

These values have been chosen through a trial-and-error methodology with the aim of maximising the clarity of the graphs presented.
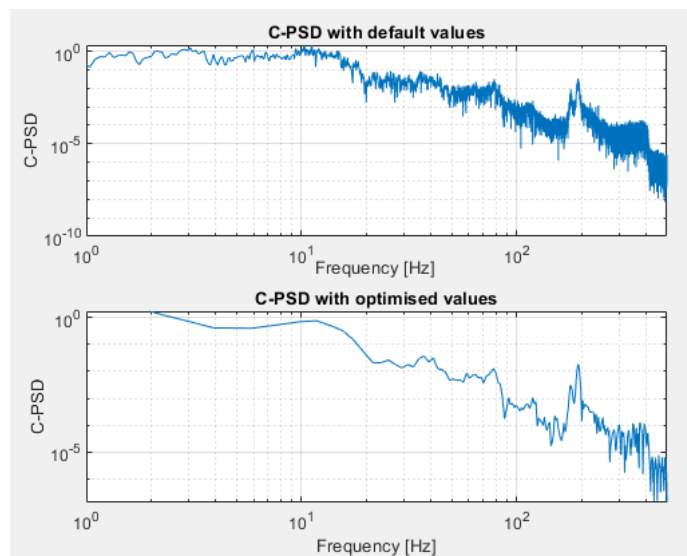

Figure 35, C-PSD comparison.

\

It is important to note that the absolute value of the calculated C-PSD has been graphed to facilitate the utilization of a double logarithmic scale in the Fig. [35] and for subsequent data analysis. Prior to presenting the conducted analysis, it is worth emphasizing that, as the cross-spectral density involves a dual signal technique, two signal pairs were examined. The initial pair under analysis comprises the force transducer signal and the accelerometer signal located on the top mount of the same wheel. Meanwhile, the second pair involves the accelerometer signal at the centre of the wheel and the previously employed signal from the top mount. Having laid the foundation for the analysis, the exploration of the graphical representation of the cross-spectral density can proceed.
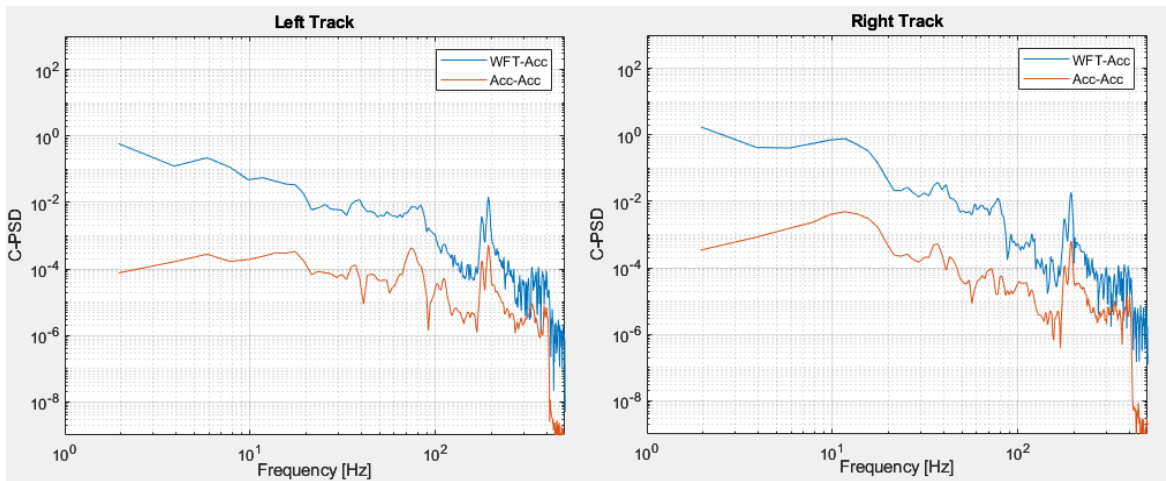
Figure 36, C-PSD of the two low speed tracks.

Therefore, the presentation of the results in this paragraph begins, as in the previous analysis, with the two single-speed tracks at lower speeds. In Fig. [36] are shown the computed Cross spectral densities, considering two cases. The blue line was obtained by measuring the mutual energy of the signal coming from the WFT and the signal coming from the accelerator positioned on the top mount, while the orange line uses the signal coming from the accelerometer at the wheel hub. It should be noted that the peak of the mutual power of these signals occurs around the pivotal frequency of 200Hz. This observation serves to unequivocally affirm the intrinsic relevance of these signals within the expansive framework of the entire vehicle system. The peak

\

identified at 200Hz not only indicates a critical resonance point, but also underlines the consequent impact of these signals on the overall dynamics of the vehicular system.
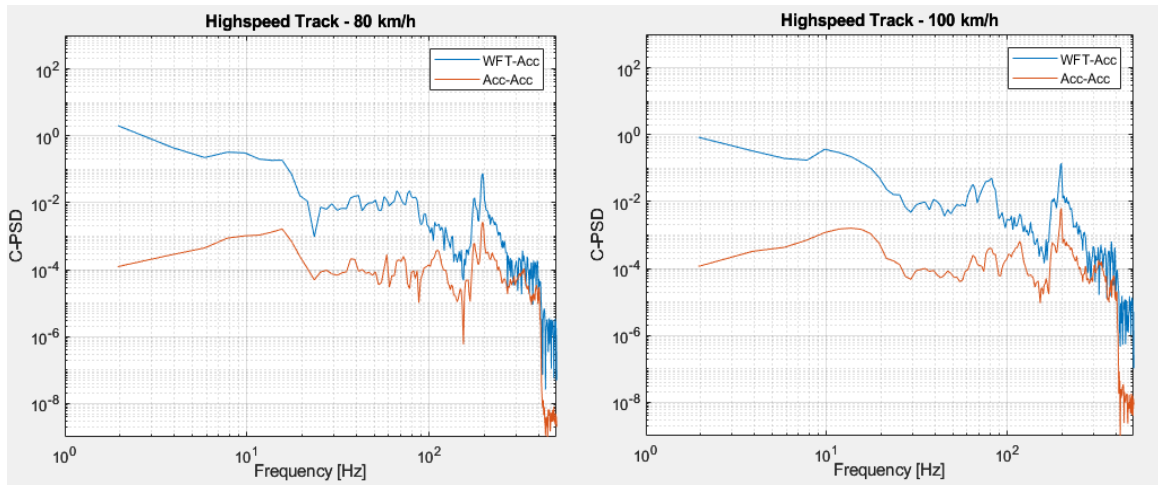
Figure 37, C-PSD of the highspeed track at different speeds.

The importance of the peak at 200 Hz is further confirmed by measurements from the track with different types of roughness being present and standing out from the energy present at all other frequencies.
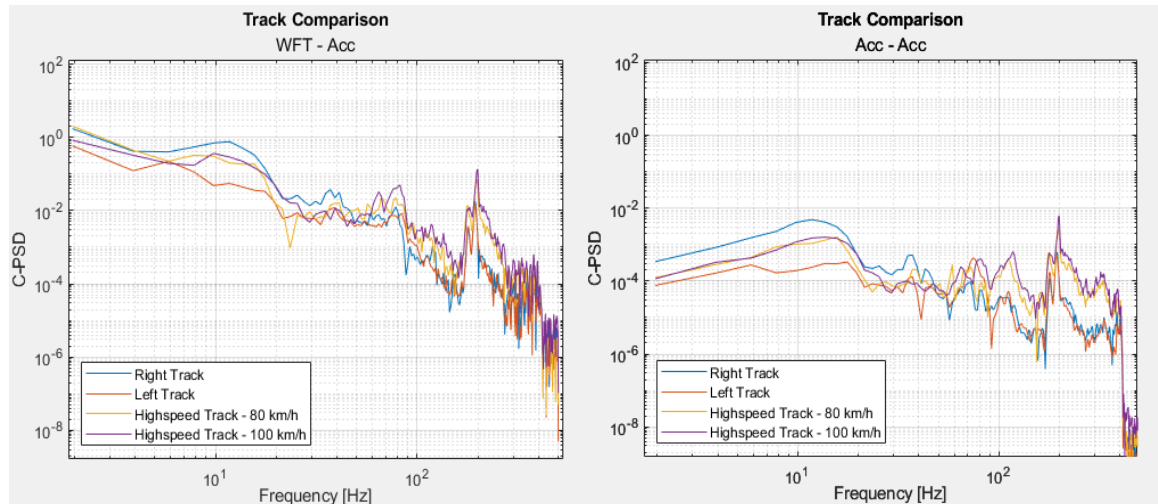
Figure 38, C-PSD comparison of all the tracks.

Finally, it is crucial to highlight the substantial similarity in the results found between force transducers and accelerometers, reinforcing the importance of being able to validate measurements made using a vehicle without wheel force transducers. Fig. [38]

\

compares all the track in the same graph for both the couple of signals analysed, and it does not show any particular discrepancies between the two cases. Therefore, it is confirmed that it is essential to conduct comparative analyses using vehicles without WFT, in order to ensure the generalisability of the results and to consolidate the validity of the results obtained in this analysis.

5.3 Magnitude Squared Coherence

This chapter explores a fundamental element in the dynamic analysis of vehicular systems: the Magnitude Squared Consistency (MSC). The introduction of the MSC allows for a deeper understanding of the dynamic relationships between the different measured variables. The MSC, being a measure of coherence, proves to be an excellent tool for analysing data from the test tracks, providing, together with cross spectral density, a clear perspective on the correlation and interaction between signals. The Magnitude Squared Coherence (MSC) serves as a signal processing tool, producing real values within the range of 0 to 1, indicative of the degree of correspondence between two time-domain signals, denoted as *x(t)* and *y(t)*. In assessing the level of similarity, the algorithm scrutinizes linear dependencies within the spectral decomposition of x(t) and y(t), calculating MSC(f) values across various frequencies according to:

$$\gamma_{xy}^2(\omega) = \frac{|G_{xy}(\omega)|^2}{G_{xx}(\omega)G_{yy}(\omega)}$$

In which, G_{xy} is the cross-power spectral density of the two signals and, G_{xx} and G_{yy} the related power spectral densities.

In this specific function, MATLAB calls up the function with the command 'mscohere', which needs the same parameters specified for the calculation of the Cross spectral density, defined through the same approach involved for the previous function,

\

reaching a good trade-off between accuracy and graphical clearness. Before proceeding with data presentation, it should be pointed out that, since the output of this function is in between zero and one, it has been decided to keep the linear scale for data plotting.
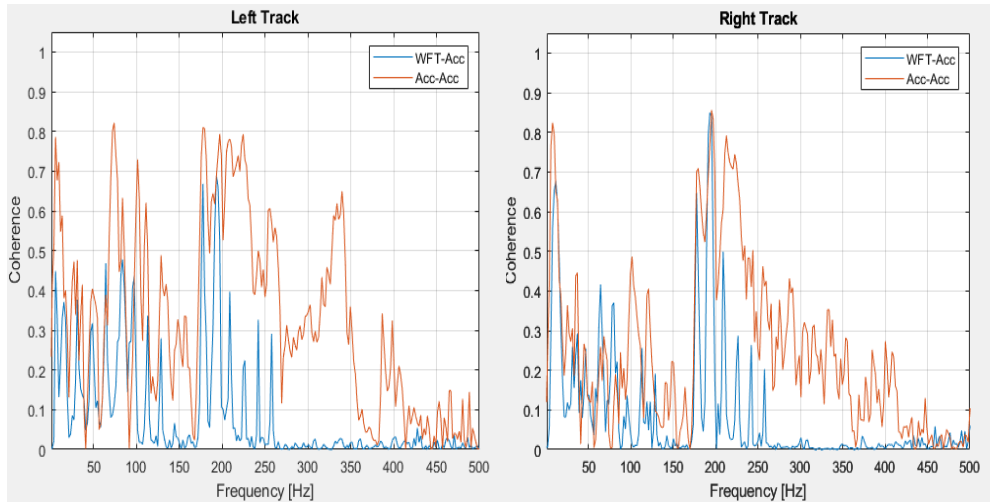

Figure 39, Magnitude squared coherence of the two low speed tracks.

The following analysis is structured similarly with the C-PSD analysis, in fact, in Fig. [39] are plotted coherence functions for both the two tracks travelled at 50 km/h, comparing at the same time the WTF-accelerometer couple and the double accelerometer pair. Thus, the preliminary observations from this analysis draw attention to a notable distinction in the calculated coherence between the two sensor pairs. A conspicuous observation is the appreciable increase in the coherence function values for the signals obtained from the accelerometers when compared to those from the Wheel Force Transducer (WFT). Specifically, in both measurement instances, the WFT and accelerometer pair exhibit singular coherence peaks within an exceptionally narrow frequency range. Conversely, the second sensor pair demonstrates a considerable widening of this frequency window, particularly evident between 150 and 250 Hz. Furthermore, the drastic drop in the value of the coherence function for the WFT-Accelerometer pair above 250 Hz is also interesting. This could indicate either a lower acquisition capacity at high frequencies, i.e. closer to the acquisition frequency, of the WFT, or as the frequency increases, the difference in the acquisition of external

\

excitations by the two sensors also increases, thereby leading to a zero correlation between the input and output of the system between the two sensors. This disparity in coherence characteristics suggests potential variations in sensor dynamics or responses, as the operation of the two sensors is different.
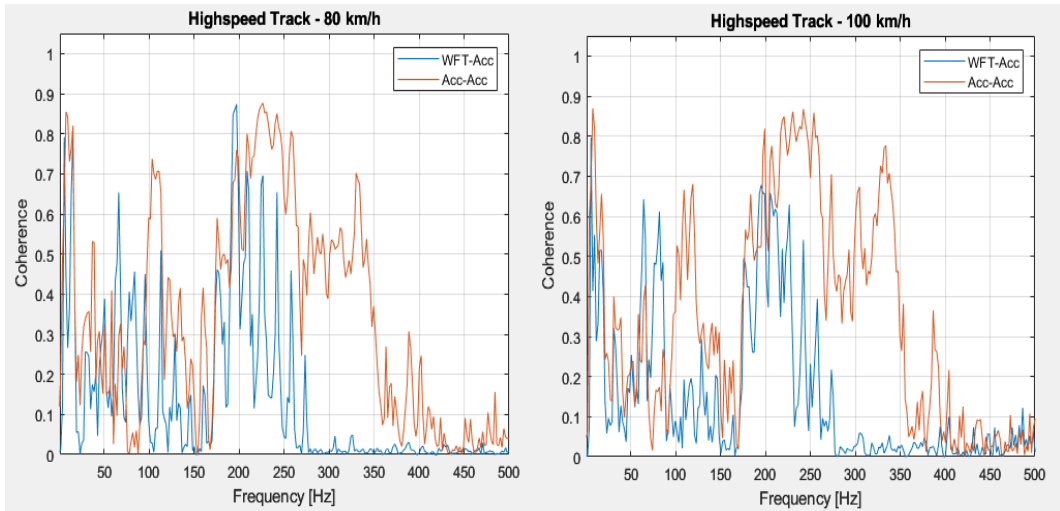
Figure 40, Magnitude squared coherence of the highspeed track at different speeds.

Moving the analysis to the highspeed tracks, the behaviour reflects the conclusions from the analysis carried out for the low-speed tracks. A noticeable difference can be seen in this case concerns a greater coherence for the pair of accelerometer signals after 250 Hz up to about 350 Hz. This window definitely shows greater coherence between the signals, while remaining below the value of 0.8, the minimum limit recognized in the literature for which the coherence function can be considered good.
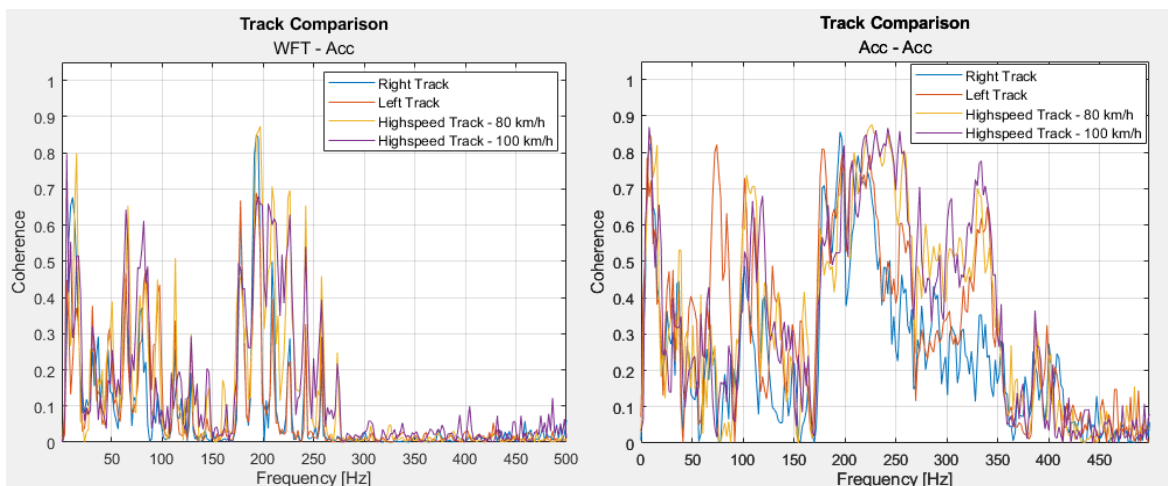
Figure 41, Comparison of all the MSC calculations.

\

In Fig. [41], the analysed pairs are divided and it is clear that the coherence function calculated for the signals both coming from the accelerometers, furthermore, between 180 Hz and 250 Hz, since the coherence function for the second pair is around 0,8 it can be stated that the suspension system exhibits characteristics akin to a linear system. Recalling the results of the previous chapters, the dominant peak, present in both PSD and C-PSD, fell within this window of greatest coherence, further underlining its importance with regard to longitudinal dynamics analysis.

\

Chapter 6

Conclusions and future works

6.1 Conclusions

First of all, the consistency of the measurements made was demonstrated by comparing the various time-domain signals available and comparing them with what is stated on the website of the test track owner (Michelin) from which most of the measurements analysed in this thesis came. The robust consistency allowed for the continuation of analyses and comparisons between the wheel force transducers (WFT) and accelerometers in the frequency domain. This aspect serves as the focal point of the entire study, as it enables an exploration of the energy distribution from the road across the frequency spectrum, scaled according to the Nyquist frequency (500 Hz). For both sensors the PSD was quite similar, in fact the macroscopic behaviour of the system was found to be similar in both cases. an interesting feature is the presence of the moving peak, which is related to the frequency of wheel rotation. This peculiarity is present only in all the WFT's measurements, indicating a possible imbalance of the wheel, perhaps due to inaccurate mounting of the sensor adapter. Moving to the dual signal analysis techniques, the results from C-PSD computation confirms what already stated for PSD, since it still computes the energy content, but this time is the mutual energy of two signals. What adds different information is the calculation of the magnitude squared coherence in that it 'measures' the linearity of the system across the frequency spectrum by analysing the input and output signals of a system. in this case, there is a greater difference between the pairs of signals analysed and greater correlation between the pair of signals from the accelerometers.

\

6.2 Future works

As already described throughout this thesis, the data provided comes from measurements that have already been taken and without the possibility of adding tests. Precisely this is one of the weak points concerning the data itself, restricting the possibility of further investigating the performance of force transducers for comfort purposes.

Analysing the evidence, the proposed future tests are:

- To be able to use cruise control for greater speed stability.
- Running the test tracks at different speeds, starting from low speeds, where the tyre behaves closer to a linear system, up to higher speeds, around 80 km/h
- being able to carry out 'dual' tests, both with the vehicle fitted with WFTs and with the vehicle fitted with accelerometers only. This would highlight any differences due to possible variations in unsprang mass.

an example would be:

on a single test track, similar to a low-speed track presented in this thesis, run from 5 km/h and with each new measurement increase the speed by 5 km/h until 60/70 km/h is reached. These measurements should be made both with WFT and without, having the ability to compare and quantify any differences due to the presence of the force transducers at the wheels.

\

\

References

[1] İ. Karen & N. Kaya & F. Öztürk & İ. Korkmaz & M. Yıldızhan & A. Yurttaş, "A design tool to evaluate the vehicle ride comfort characteristics: modeling, physical testing, and analysis". Int J Adv Manuf Technol (2012) 60:755–763 DOI 10.1007/s00170-011-3592.

[2] Thom, B., Blanco, D., and Caltagirone, E., "Contributiuon Analysis for Ride Comfort Evaluations," SAE Technical Paper 2023-01-1144, 2023, doi:10.4271/2023-01-1144.

[3] Freeman, T. and Cerrato, G., "Source-Path-Contribution Methodologies across a Wide Range of Product Types," SAE Int. J. Passeng. Cars - Mech. Syst. 8, no. 2 (2015): 762-766, https://doi.org/10.4271/2015-01-2360.

[4] Burkard H. Sidler A. Wolfer P., "Dynamic Wheel Load Measurements on Real Road Surfaces - What Accuracy to Expect?", SAE Int. J. Passeng. Cars, 2001-01-0745

[5] Shawn S. You, "Effect of Added Mass of Spindle Wheel Force Transducer on Vehicle Dynamic Response", SAE international, doi:10.4271/2012-01-021

[6] Sommerfeld, J., and Meyer, R., "Correlation and Accuracy of a Wheel Force Transducer as Developed and Tested on a Flat-Trac® Tire Test System," SAE Technical Paper 1999-01-0938, 1999, doi:10.4271/1999-01-0938.

[7] J. S. Lin and Kui-Sun Yim, "Application of Random Vibration Test Methods for Automotive Subsystems Using Power Spectral Density", SAE 2000 World Congress, SAE Technical Paper 2000-01-1331

[8] Vella, A.D., Vigliani, A., Tota, A., and Lisitano, D., "Experimental Ride Comfort Analysis of an Electric Light Vehicle in Urban Scenario," SAE Technical Paper 2020-01-1086, 2020, doi:10.4271/2020-01-1086.

[9] Perry Gu, Z. C. Feng, "Modelling and Experimental Verification of Vibration and Noise Caused by the Cavity Modes of a Rolling Tire under Static Loading", SAE Technical Papers, doi: 10.4271/2011-01-1581.

[10] Fundamentals of Noise and Vibration Analysis for Engineers, M. P. Norton and D. G. Karczub.

[11] https://it.mathworks.com/